

Dynamics of annihilation. I. Linearized Boltzmann equation and hydrodynamics

María Isabel García de Soria,¹ Pablo Maynar,^{2,3} Grégory Schehr,² Alain Barrat,² and Emmanuel Trizac¹

¹LPTMS (CNRS UMR 8626), Université Paris-Sud, Orsay Cedex, F-91405, France

²Laboratoire de Physique Théorique (CNRS UMR 8627), Université Paris-Sud, Bâtiment 210, 91405 Orsay Cedex, France

³Física Teórica, Universidad de Sevilla, Apartado de Correos 1065, E-41080, Sevilla, Spain

(Received 17 January 2008; published 28 May 2008)

We study the nonequilibrium statistical mechanics of a system of freely moving particles, in which binary encounters lead either to an elastic collision or to the disappearance of the pair. Such a system of *ballistic annihilation* therefore constantly loses particles. The dynamics of perturbations around the free decay regime is investigated using the spectral properties of the linearized Boltzmann operator, which characterize linear excitations on all time scales. The linearized Boltzmann equation is solved in the hydrodynamic limit by a projection technique, which yields the evolution equations for the relevant coarse-grained fields and expressions for the transport coefficients. We finally present the results of molecular dynamics simulations that validate the theoretical predictions.

DOI: [10.1103/PhysRevE.77.051127](https://doi.org/10.1103/PhysRevE.77.051127)

PACS number(s): 02.50.-r, 51.10.+y, 05.20.Dd, 82.20.Nk

I. INTRODUCTION

Understanding the differences and similarities between a flow of macroscopic grains and that of an ordinary liquid is an active field of research [1,2]. From a fundamental perspective, it is tempting to draw a correspondence between the grains of the former and the atoms of the latter in order to make use of the powerful tools of statistical mechanics to derive a large-scale description for the various fields of interest, such as the local density of grains. A key difference between a granular system and an ordinary liquid is that collisions between macroscopic grains dissipate energy, due to the redistribution of translational kinetic energy into internal modes. This simple fact has far-reaching consequences [2,3], but also poses an *a priori* serious problem concerning the validity of the procedure leading to the hydrodynamic description. Indeed, the standard approach retains in the coarse-grained description only those fields associated with quantities that are conserved in collisions (such as density and momentum). There is however good evidence—both numerical and theoretical—that, in the granular case, a relevant description should include the kinetic temperature field, defined as the kinetic energy density ([2,4,5] and references therein), which is therefore not associated with a conserved quantity.

Our purpose here is to test a hydrodynamic description with suitable coarse-grained fields, for a model system where not only is the kinetic energy not conserved during binary encounters, but neither are the number of particles and the linear momentum. The ballistic annihilation model [6–11] provides a valuable candidate: in this model, each particle moves freely (ballistically) until it meets another particle; such binary encounters lead to the annihilation of the colliding pair of particles. In addition, we introduce a parameter $0 \leq p \leq 1$ that may be thought of as a measure of the distance to equilibrium, so that an ensemble of spherical particles in dimension d undergoing ballistic motion either annihilate upon contact (with probability p) or scatter elastically (with probability $1-p$). For the corresponding probabilistic ballistic annihilation model, the Chapman-Enskog [12] scheme was applied recently [13]. The hydrodynamic equations were derived and explicit formulas for the transport coefficients

obtained. Our goal here is twofold. First, we would like to shed light on the context and limitations of the derivation, by obtaining the hydrodynamic description directly from the linearized Boltzmann equation. Second, we aim at putting to the test the theoretical framework thereby obtained by careful comparison with numerical simulations of the annihilation process. For granular gas dynamics, the same program is quite complete, although challenges remain [1,2]. The objective here is to initiate a similar formulation for the ballistic annihilation model in view of a more stringent test of the hydrodynamic machinery.

The paper is organized as follows. We start in Sec. II with a reminder of results derived in Refs. [9,10]. The kinetic description adopted is that of the Boltzmann equation, since it has been shown that for $p=1$ (all collision events leading to annihilation), the underlying molecular chaos closure provides an exact description at long times, provided the space dimension d is strictly larger than 1 [10]. We may assume that the same holds for an arbitrary but nonvanishing value of p , since the density is then still a decreasing function of time. The focus is here on an unforced system, which is characterized by an algebraic decay with time of the total density and kinetic energy density (homogeneous decay state) [9,10]. More precisely, we are interested in small perturbations around this state, so that the Boltzmann equation will be subsequently linearized. After having identified the operator that generates the dynamics of fluctuations, attention will be paid in Sec. III to its spectral properties. This will provide the basis for finding in Sec. IV the evolution equations for the hydrodynamic fields (i.e., those chosen for the coarse-grained description) and for obtaining explicit formulas for the transport coefficients. Finally, our predictions will be confronted in Sec. V against extensive molecular dynamics simulations. Such a comparison is an essential step in testing the foundations of the hydrodynamic treatment.

II. THE BOLTZMANN EQUATION APPROACH TO THE HOMOGENEOUS DECAY STATE

A. Nonlinear description

The Boltzmann equation describes the time evolution of the one-particle distribution function $f(\mathbf{r}, \mathbf{v}_1, t)$. For a system

of smooth hard disks or spheres of mass m and diameter σ , which annihilate with probability p or collide elastically with probability $1-p$, it has the form

$$\left(\frac{\partial}{\partial t} + \mathbf{v}_1 \cdot \nabla\right) f(\mathbf{r}, \mathbf{v}_1, t) = p J_a[f|f] + (1-p) J_c[f|f], \quad (1)$$

where the annihilation operator J_a is defined by [10]

$$J_a[f|g] = -\sigma^{d-1} \int d\mathbf{v}_2 \int d\hat{\boldsymbol{\sigma}} \Theta(\mathbf{v}_{12} \cdot \hat{\boldsymbol{\sigma}}) \times (\mathbf{v}_{12} \cdot \hat{\boldsymbol{\sigma}}) f(\mathbf{r}, \mathbf{v}_1, t) g(\mathbf{r}, \mathbf{v}_2, t). \quad (2)$$

The elastic collision operator J_c reads [14,15]

$$J_c[f|g] = \sigma^{d-1} \int d\mathbf{v}_2 \int d\hat{\boldsymbol{\sigma}} \Theta(\mathbf{v}_{12} \cdot \hat{\boldsymbol{\sigma}}) (\mathbf{v}_{12} \cdot \hat{\boldsymbol{\sigma}}) (b_\sigma^{-1} - 1) \times f(\mathbf{r}, \mathbf{v}_1, t) g(\mathbf{r}, \mathbf{v}_2, t), \quad (3)$$

with $\mathbf{v}_{12} = \mathbf{v}_1 - \mathbf{v}_2$, Θ the Heaviside step function, $\hat{\boldsymbol{\sigma}}$ a unit vector joining the centers of the two particles at contact, and b_σ^{-1} an operator replacing all the velocities \mathbf{v}_1 and \mathbf{v}_2 appearing in its argument by their precollisional values \mathbf{v}_1^* and \mathbf{v}_2^* , given by

$$b_\sigma^{-1} \mathbf{v}_1 = \mathbf{v}_1^* = \mathbf{v}_1 - (\mathbf{v}_{12} \cdot \hat{\boldsymbol{\sigma}}) \hat{\boldsymbol{\sigma}}, \quad (4)$$

$$b_\sigma^{-1} \mathbf{v}_2 = \mathbf{v}_2^* = \mathbf{v}_2 + (\mathbf{v}_{12} \cdot \hat{\boldsymbol{\sigma}}) \hat{\boldsymbol{\sigma}}. \quad (5)$$

We assume that the system can be characterized macroscopically by coarse-grained (hydrodynamiclike) fields, which we define as in standard kinetic theory in terms of the local velocity distribution function $f(\mathbf{r}, \mathbf{v}, t)$,

$$n(\mathbf{r}, t) = \int d\mathbf{v} f(\mathbf{r}, \mathbf{v}, t), \quad (6)$$

$$n(\mathbf{r}, t) \mathbf{u}(\mathbf{r}, t) = \int d\mathbf{v} \mathbf{v} f(\mathbf{r}, \mathbf{v}, t), \quad (7)$$

$$\frac{d}{2} n(\mathbf{r}, t) T(\mathbf{r}, t) = \int d\mathbf{v} \frac{m}{2} V^2 f(\mathbf{r}, \mathbf{v}, t), \quad (8)$$

where $n(\mathbf{r}, t)$, $\mathbf{u}(\mathbf{r}, t)$, and $T(\mathbf{r}, t)$ are the local number density, velocity, and temperature, respectively. We have introduced here $\mathbf{V} = \mathbf{v} - \mathbf{u}$, the velocity of the particle relative to the local velocity flow. We stress that the temperature defined has a kinetic meaning only, but lacks a thermodynamic interpretation. It seems natural to consider these fields, as they are the usual hydrodynamical fields of the equilibrium system (with $p=0$). It is, however, not obvious at this point that restricting our coarse-grained description to the above three fields provides a relevant and consistent framework. A major goal of this paper is to provide strong hints that this is indeed the case. We will show in particular that closed equations can be obtained for these fields in the appropriate time and length scales, under reasonable assumptions.

The Boltzmann equation (1) admits a homogeneous scaling solution f_H in which all the time dependence is embedded in the hydrodynamic fields, with the further simplifica-

tion that those fields are position independent. The existence of this regime could not be shown rigorously, but, numerically, such a scaling solution quickly emerges from an arbitrary initial condition [9,10]. It has the form [10]

$$f_H(\mathbf{v}, t) = \frac{n_H(t)}{v_H(t)^d} \chi_H(\mathbf{c}) \quad \text{with} \quad \mathbf{c} = \frac{\mathbf{v}}{v_H(t)}, \quad (9)$$

where

$$v_H(t) = \left(\frac{2T_H(t)}{m}\right)^{1/2} \quad (10)$$

is the ‘‘thermal’’ (root-mean-square) velocity and $\chi_H(\mathbf{c})$ is an isotropic function depending only on the modulus $c = |\mathbf{c}|$ of the rescaled velocity. By taking moments in the Boltzmann equation and using the scaling (9), it can be seen that the homogeneous density and temperature obey the equations [13]

$$\frac{\partial n_H(t)}{\partial t} = -p \nu_H(t) \zeta_n n_H(t), \quad (11)$$

$$\frac{\partial T_H(t)}{\partial t} = -p \nu_H(t) \zeta_T T_H(t), \quad (12)$$

where we have introduced the collision frequency of the corresponding hard sphere fluid in equilibrium (with the same temperature and density),

$$\nu_H(t) = \frac{n_H(t) T_H^{1/2}(t) \sigma^{d-1}}{m^{1/2}} \frac{8\pi^{d-1/2}}{(d+2)\Gamma(d/2)}, \quad (13)$$

and the dimensionless decay rates ζ_n and ζ_T , which are functionals of the distribution function,

$$p \zeta_n = -\frac{\gamma}{2} \int d\mathbf{c}_1 \int d\mathbf{c}_2 T(\mathbf{c}_1, \mathbf{c}_2) \chi_H(\mathbf{c}_1) \chi_H(\mathbf{c}_2), \quad (14)$$

$$p \zeta_T = -\frac{\gamma}{2} \int d\mathbf{c}_1 \int d\mathbf{c}_2 \left(\frac{2c_1^2}{d} - 1\right) T(\mathbf{c}_1, \mathbf{c}_2) \chi_H(\mathbf{c}_1) \chi_H(\mathbf{c}_2). \quad (15)$$

In these expressions, γ is a quantity that does not depend on time, which reads

$$\gamma = \frac{2n_H(t)v_H(t)\sigma^{d-1}}{v_H(t)} = \frac{(d+2)\sqrt{2}\Gamma(d/2)}{4\pi^{(d-1)/2}}, \quad (16)$$

and the binary collision operator $T(\mathbf{c}_1, \mathbf{c}_2)$, which should not be confused with the temperature, takes the form

$$T(\mathbf{c}_1, \mathbf{c}_2) = \int d\hat{\boldsymbol{\sigma}} \Theta(\mathbf{c}_{12} \cdot \hat{\boldsymbol{\sigma}}) (\mathbf{c}_{12} \cdot \hat{\boldsymbol{\sigma}}) [(1-p)b_\sigma^{-1} - 1]. \quad (17)$$

Finally, we can write an equation for the scaled distribution function $\chi_H(\mathbf{c})$ in terms of the coefficients and operators defined above:

$$\begin{aligned}
& p \left((d\zeta_T - 2\zeta_n) + \zeta_T \mathbf{c}_1 \cdot \frac{\partial}{\partial \mathbf{c}_1} \right) \chi_H(\mathbf{c}_1) \\
&= \gamma \int d\mathbf{c}_2 T(\mathbf{c}_1, \mathbf{c}_2) \chi_H(\mathbf{c}_1) \chi_H(\mathbf{c}_2). \quad (18)
\end{aligned}$$

The operator b_σ^{-1} in the last equation is defined again by Eq. (4), but substituting $(\mathbf{v}_1, \mathbf{v}_2)$ by $(\mathbf{c}_1, \mathbf{c}_2)$.

Although an exact and explicit solution of Eq. (18) is not known, its behavior at large and small velocities has been determined [9,10]. In this work we will use the approximate form of the distribution function in the so-called first Sonine approximation (an expansion around a Gaussian functional form; see Appendix A), which is valid for velocities in the thermal region, and all the functionals of $\chi_H(\mathbf{c})$, that is the decay rates and the transport coefficients, will be evaluated in this approximation [9,16].

B. Linearized Boltzmann equation

In the remainder, we consider a situation where the system is very close to the homogeneous decay state, so that we can write

$$f(\mathbf{r}, \mathbf{v}_1, t) = f_H(\mathbf{v}_1, t) + \delta f(\mathbf{r}, \mathbf{v}_1, t), \quad |\delta f(\mathbf{r}, \mathbf{v}_1, t)| \ll f_H(\mathbf{v}_1, t). \quad (19)$$

Substitution of Eq. (19) into the Boltzmann equation (1), keeping only linear terms in δf , yields

$$\begin{aligned}
\left(\frac{\partial}{\partial t} + \mathbf{v}_1 \cdot \nabla \right) \delta f(\mathbf{r}, \mathbf{v}_1, t) &= p(J_a[\delta f|f_H] + J_a[f_H|\delta f]) + (1-p) \\
&\times (J_c[\delta f|f_H] + J_c[f_H|\delta f]), \quad (20)
\end{aligned}$$

Given the scaling form of f [Eq. (9)], it is convenient to introduce as well the scaled deviation of the distribution function, $\delta\chi$, as follows:

$$\delta f(\mathbf{r}, \mathbf{v}_1, t) = \frac{n_H(t)}{v_H(t)^d} \delta\chi(\mathbf{r}, \mathbf{c}_1, \tau). \quad (21)$$

Moreover, Eqs. (11) and (12) suggest use of the dimensionless time scale τ defined by

$$\tau = \frac{1}{2} \int_0^t dt' v_H(t'), \quad (22)$$

which counts the number of collisions per particle in the time interval $[0, t]$. Combining Eq. (13) together with Eqs. (11) and (12) yields immediately $v_H(t) = [1/v_H(0) + p(\zeta_n + \zeta_T/2)t]^{-1}$ and thus

$$\tau = \frac{1}{p(2\zeta_n + \zeta_T)} \ln[1 + v_H(0)p(\zeta_n + \zeta_T/2)t]. \quad (23)$$

In this time scale τ (22), these Eqs. (11) and (12) are easily integrated, yielding

$$n_H(\tau) = n_H(0) \exp(-2p\zeta_n\tau), \quad T_H(\tau) = T_H(0) \exp(-2p\zeta_T\tau), \quad (24)$$

and power law behaviors in time t , $n_H(t) \propto t^{-2\zeta_n/(2\zeta_n + \zeta_T)}$ and $T_H(t) \propto t^{-2\zeta_T/(2\zeta_n + \zeta_T)}$ at large times $t \gg 1$. It proves also convenient to introduce Fourier components [with the notation $h_{\mathbf{k}} = \int d\mathbf{r} \exp^{-i\mathbf{k}\cdot\mathbf{r}} h(\mathbf{r})$] so that the evolution equation for a general \mathbf{k} component of $\delta\chi$ is, in the τ time scale,

nient to introduce Fourier components [with the notation $h_{\mathbf{k}} = \int d\mathbf{r} \exp^{-i\mathbf{k}\cdot\mathbf{r}} h(\mathbf{r})$] so that the evolution equation for a general \mathbf{k} component of $\delta\chi$ is, in the τ time scale,

$$\frac{\partial}{\partial \tau} \delta\chi_{\mathbf{k}}(\mathbf{c}_1, \tau) = [\Lambda(\mathbf{c}_1) - i l_H(\tau) \mathbf{k} \cdot \mathbf{c}_1] \delta\chi_{\mathbf{k}}(\mathbf{c}_1, \tau). \quad (25)$$

In this equation, the time-dependent length scale $l_H = 2v_H(\tau)/v_H(\tau)$ is proportional to the instantaneous mean free path [$l_H(\tau) \propto n_H^{-1}(\tau)$; see Eq. (13)] and the homogeneous scaled Boltzmann linear operator reads

$$\begin{aligned}
\Lambda(\mathbf{c}_1) h(\mathbf{c}_1) &= \gamma \int d\mathbf{c}_2 T(\mathbf{c}_1, \mathbf{c}_2) (1 + \mathcal{P}_{12}) \chi_H(\mathbf{c}_1) h(\mathbf{c}_2) \\
&+ p(2\zeta_n - d\zeta_T) h(\mathbf{c}_1) - p\zeta_T \mathbf{c}_1 \cdot \frac{\partial}{\partial \mathbf{c}_1} h(\mathbf{c}_1). \quad (26)
\end{aligned}$$

In this expression, the permutation operator \mathcal{P}_{12} interchanges the labels of particles 1 and 2 and subsequently allows for more compact notations. In the present representation, all the time dependence due to the reference state is absorbed in the mean free path, obtained from $l_H(\tau) \propto n_H^{-1}(\tau)$ as

$$l_H(\tau) = l_H(0) \exp(2p\zeta_n\tau), \quad (27)$$

which, as expected, is an increasing function of time.

C. Linearized hydrodynamic equations around the homogeneous decay state

Let us define the relative deviations of the hydrodynamic fields from their homogeneous values by

$$\rho(\mathbf{r}, \tau) \equiv \frac{\delta n(\mathbf{r}, \tau)}{n_H(\tau)} = \int d\mathbf{c} \delta\chi(\mathbf{r}, \mathbf{c}, \tau), \quad (28)$$

$$\mathbf{w}(\mathbf{r}, \tau) \equiv \frac{\delta \mathbf{u}(\mathbf{r}, \tau)}{v_H(\tau)} = \int d\mathbf{c} \mathbf{c} \delta\chi(\mathbf{r}, \mathbf{c}, \tau), \quad (29)$$

$$\theta(\mathbf{r}, \tau) \equiv \frac{\delta T(\mathbf{r}, \tau)}{T_H(\tau)} = \int d\mathbf{c} \left(\frac{2c^2}{d} - 1 \right) \delta\chi(\mathbf{r}, \mathbf{c}, \tau), \quad (30)$$

where $\delta y(\mathbf{r}, \tau) \equiv y(\mathbf{r}, \tau) - y_H(t)$ denotes the deviation of a local macroscopic variable, $y(\mathbf{r}, \tau)$, from its homogeneous decay state value, $y_H(t)$. Taking velocity moments in the Boltzmann equation (25), we obtain the linearized balance equation for the \mathbf{k} components of the hydrodynamic fields:

$$\left(\frac{\partial}{\partial \tau} - 2p\zeta_n \right) \rho_{\mathbf{k}} + i l_H(\tau) \mathbf{k} \cdot \mathbf{w}_{\mathbf{k}} - p \delta\zeta_n [\delta\chi_{\mathbf{k}}] = 0, \quad (31)$$

$$\begin{aligned}
\left(\frac{\partial}{\partial \tau} - p(2\zeta_n + \zeta_T) \right) \mathbf{w}_{\mathbf{k}} + \frac{i}{2} l_H(\tau) \mathbf{k} (\rho_{\mathbf{k}} + \theta_{\mathbf{k}}) \\
+ i l_H(\tau) \mathbf{k} \cdot \mathbf{\Pi} [\delta\chi_{\mathbf{k}}] - p \delta\zeta_u [\delta\chi_{\mathbf{k}}] = 0, \quad (32)
\end{aligned}$$

$$\left(\frac{\partial}{\partial \tau} - 2p(\zeta_n + \zeta_T)\right)\theta_{\mathbf{k}} - 2p\zeta_T\rho_{\mathbf{k}} + i\frac{2}{d}l_H(\tau)\mathbf{k} \cdot (\mathbf{w}_{\mathbf{k}} + \phi[\delta\chi_{\mathbf{k}}]) - p\delta\zeta_T[\delta\chi_{\mathbf{k}}] = 0. \quad (33)$$

Here, we have introduced the traceless pressure tensor and the heat flux as

$$\mathbf{\Pi}[\delta\chi_{\mathbf{k}}] = \int d\mathbf{c} \mathbf{\Delta}(\mathbf{c}) \delta\chi_{\mathbf{k}}(\mathbf{c}, \tau), \quad (34)$$

$$\phi[\delta\chi_{\mathbf{k}}] = \int d\mathbf{c} \mathbf{\Sigma}(\mathbf{c}) \delta\chi_{\mathbf{k}}(\mathbf{c}, \tau), \quad (35)$$

where $\mathbf{\Delta}$ and $\mathbf{\Sigma}$ are defined as

$$\Delta_{ij}(\mathbf{c}) = c_i c_j - \frac{c^2}{d} \delta_{ij}, \quad (36)$$

$$\mathbf{\Sigma}(\mathbf{c}) = \left(c^2 - \frac{d+2}{2}\right)\mathbf{c}, \quad (37)$$

and the functionals

$$p\delta\zeta_n[\delta\chi] = \gamma \int d\mathbf{c}_1 \int d\mathbf{c}_2 T(\mathbf{c}_1, \mathbf{c}_2) (1 + \mathcal{P}_{12}) \chi_H(\mathbf{c}_1) \delta\chi_{\mathbf{k}}(\mathbf{c}_2, \tau), \quad (38)$$

$$p\delta\zeta_{ul}[\delta\chi] = \gamma \int d\mathbf{c}_1 \int d\mathbf{c}_2 \mathbf{c}_1 T(\mathbf{c}_1, \mathbf{c}_2) (1 + \mathcal{P}_{12}) \times \chi_H(\mathbf{c}_1) \delta\chi_{\mathbf{k}}(\mathbf{c}_2, \tau), \quad (39)$$

$$p\delta\zeta_T[\delta\chi] = \gamma \int d\mathbf{c}_1 \int d\mathbf{c}_2 \left(\frac{2c_1^2}{d} - 1\right) T(\mathbf{c}_1, \mathbf{c}_2) \times (1 + \mathcal{P}_{12}) \chi_H(\mathbf{c}_1) \delta\chi_{\mathbf{k}}(\mathbf{c}_2, \tau). \quad (40)$$

The previous analysis therefore amounts to obtaining a set of complicated equations expressing the evolution of the hydrodynamic fields as a function of the rescaled homogeneous distribution function χ_H and the perturbation $\delta\chi$. In order to obtain a closed set of equations for the hydrodynamic fields (31)–(33), we need therefore to express the functionals $\mathbf{\Pi}$, ϕ , $\delta\zeta_n$, $\delta\zeta_{ul}$, and $\delta\zeta_T$, in terms of the hydrodynamic fields themselves. We will see in the next section that, as long as we can treat $l_H(\tau)\mathbf{k}$ as a small parameter and if the linear Boltzmann operator has some specific properties, it is possible to carry out this program and to close the linear hydrodynamic equations. However, since the mean free path $l_H(\tau)$ increases with time [Eq. (27)], the requirement of a small $l_H(\tau)\mathbf{k}$ is necessarily limited to a time window depending on both \mathbf{k} and the probability of annihilation p . An upper bound for this window is provided by the time when the mean free path becomes of the order of the system size.

III. SOLUTION OF THE LINEARIZED BOLTZMANN EQUATION

In this section we explore the solutions to the linearized Boltzmann equation (25) and establish some properties of

the homogeneous linear Boltzmann operator that will be essential for the coarse-grained description. From the expression of the linearized Boltzmann equation, we can identify the operator $\Lambda - i\mathbf{k} \cdot \mathbf{c} l_H(\tau)$ as the “generator of the dynamic” of $\delta\chi_{\mathbf{k}}$. As we are interested in the solutions of this equation in the hydrodynamic regime (large enough scales), it is convenient to study first the eigenvalue problem of the homogeneous linear Boltzmann operator. The inhomogeneous term will be treated perturbatively later on.

A. Hydrodynamic eigenfunctions of Λ

Let us consider the eigenvalue problem of the homogeneous linear Boltzmann operator Λ ,

$$\Lambda(\mathbf{c}) \xi_{\beta}(\mathbf{c}) = \lambda_{\beta} \xi_{\beta}(\mathbf{c}). \quad (41)$$

Finding all the solutions of this equation is an insurmountable task. Nevertheless, it is possible to obtain some particular solutions, which will turn out to be the relevant ones in the hydrodynamic regime. The problem will be posed in a Hilbert space of functions of \mathbf{c} with scalar product given by

$$\langle g|h \rangle = \int d\mathbf{c} \chi_H^{-1}(\mathbf{c}) g^*(\mathbf{c}) h(\mathbf{c}), \quad (42)$$

where g^* denotes the complex conjugate of g .

Of particular interest here are the eigenfunctions and eigenvalues associated with linear hydrodynamics. Following [17,18], we use the fact that the homogeneous decay state is parametrized by the hydrodynamic fields n_H , T_H , and \mathbf{u}_H . Writing the Boltzmann equation satisfied by χ_H and differentiating it with respect to these fields allows one to obtain three exact relations from which one can extract eigenfunctions of the linearized Boltzmann collision operator. In Appendix B, we show that the functions

$$\xi_1(\mathbf{c}) = \chi_H(\mathbf{c}) + \frac{\partial}{\partial \mathbf{c}} \cdot [\mathbf{c} \chi_H(\mathbf{c})], \quad (43)$$

$$\xi_2(\mathbf{c}) = z \chi_H(\mathbf{c}) - \frac{\partial}{\partial \mathbf{c}} \cdot [\mathbf{c} \chi_H(\mathbf{c})], \quad (44)$$

$$\xi_3(\mathbf{c}) = -\frac{\partial}{\partial \mathbf{c}} \chi_H(\mathbf{c}), \quad (45)$$

with $z = 2\zeta_n/\zeta_T$, are solutions of Eq. (41), with eigenvalues

$$\lambda_1 = 0, \quad \lambda_2 = -p(\zeta_T + 2\zeta_n), \quad \lambda_3 = p\zeta_T, \quad (46)$$

respectively, λ_3 being d -fold degenerate. Although we cannot prove in general that these eigenvalues are indeed the hydrodynamic ones (i.e., the upper part of the spectrum), we will assume that this is the case; the self-consistency of the approach and comparison with numerical simulations will validate this assumption. Interestingly, in the particular case of Maxwell molecules where the full spectrum of Λ may be computed exactly (see Appendix C), it appears that the above “hydrodynamic” modes dominate at long times, provided that $p < 1/4$. For larger values of p , the “kinetic” mode with largest eigenvalue decays more slowly than one of the three hydrodynamic modes.

As a consequence of the non-Hermitian character of the operator Λ , the functions $\{\xi_\beta\}_{\beta=1,\dots,3}$ are not orthogonal with respect to the scalar product defined in (42). They are nevertheless independent and, in order to define the projection onto the subspace spanned by these functions, it is necessary to introduce a set of functions $\{\bar{\xi}_\beta\}_{\beta=1,\dots,3}$ verifying the biorthonormality condition

$$\langle \bar{\xi}_\beta | \xi_{\beta'} \rangle = \delta_{\beta,\beta'}. \quad (47)$$

Although the set $\{\bar{\xi}_\beta\}_{\beta=1,\dots,3}$ is not unique, a convenient choice is given by

$$\bar{\xi}_1(\mathbf{c}) = \left(\frac{2+z}{2(1+z)} - \frac{z}{1+z} \frac{c^2}{d} \right) \chi_H(\mathbf{c}), \quad (48)$$

$$\bar{\xi}_2(\mathbf{c}) = \left(\frac{1}{2(1+z)} + \frac{1}{1+z} \frac{c^2}{d} \right) \chi_H(\mathbf{c}), \quad (49)$$

$$\bar{\xi}_3(\mathbf{c}) = \mathbf{c} \chi_H(\mathbf{c}). \quad (50)$$

Indeed, the functions $\{\bar{\xi}_\beta\}_{\beta=1,\dots,3}$ have to be linear combinations of $\chi_H(c)$, $\mathbf{c}\chi_H(c)$, and $c^2\chi_H(c)$ to ensure that projection of $\delta\chi_{\mathbf{k}}$ onto $\{\bar{\xi}_\beta\}$ yields the coarse-grained fields $\rho_{\mathbf{k}}$, $\theta_{\mathbf{k}}$, and $\mathbf{w}_{\mathbf{k}}$, or combinations thereof. The functions $\{\bar{\xi}_\beta\}_{\beta=1,\dots,3}$ span a dual subspace of that spanned by the eigenfunctions and for any linear combination of the hydrodynamic modes

$$g(\mathbf{c}) = \sum_{\beta=1}^3 a_\beta \bar{\xi}_\beta(\mathbf{c}), \quad (51)$$

the coefficients a_β are given by

$$a_\beta = \langle \bar{\xi}_\beta | g \rangle = \int d\mathbf{c} \bar{\chi}_H^{-1}(\mathbf{c}) \bar{\xi}_\beta(\mathbf{c}) g(\mathbf{c}). \quad (52)$$

In particular, the projection of the distribution function $\delta\chi_{\mathbf{k}}$ on the subspace spanned by the functions $\bar{\xi}_\beta$ is given by the coefficients

$$\{\langle \bar{\xi}_\beta | \delta\chi_{\mathbf{k}} \rangle\} = \left\{ \frac{1}{1+z} \rho_{\mathbf{k}} - \frac{z}{2(1+z)} \theta_{\mathbf{k}}, \frac{1}{1+z} \rho_{\mathbf{k}} + \frac{1}{2(1+z)} \theta_{\mathbf{k}}, \mathbf{w}_{\mathbf{k}} \right\}. \quad (53)$$

Notably, these coefficients are simply linear combinations of the hydrodynamic fields linearized around the homogeneous decay state.

B. Projection of the linearized Boltzmann equation on the hydrodynamic subspace

In this section, we study the linearized Boltzmann equation on the hydrodynamic subspace. Let us define the projectors

$$Ph(\mathbf{c}) = \sum_{\beta=1}^3 \langle \bar{\xi}_\beta | h \rangle \bar{\xi}_\beta(\mathbf{c}) \quad (54)$$

and

$$P_\perp = 1 - P, \quad (55)$$

so that any function can be decomposed as

$$h(\mathbf{c}) = Ph(\mathbf{c}) + P_\perp h(\mathbf{c}). \quad (56)$$

In the definition (54) we are considering the functions (43)–(45) and (48)–(50) defined above.

Let us now consider the function $\delta\chi_{\mathbf{k}}$. If we apply the projectors P and P_\perp to Eq. (25), we obtain the following relations:

$$\left(\frac{\partial}{\partial \tau} - P(\Lambda - il_H \mathbf{k} \cdot \mathbf{c})P \right) P \delta\chi_{\mathbf{k}} = -P il_H \mathbf{k} \cdot \mathbf{c} P_\perp \delta\chi_{\mathbf{k}} + P \Lambda P_\perp \delta\chi_{\mathbf{k}}, \quad (57)$$

$$\left(\frac{\partial}{\partial \tau} - P_\perp (\Lambda - il_H \mathbf{k} \cdot \mathbf{c}) P_\perp \right) P_\perp \delta\chi_{\mathbf{k}} = -P_\perp il_H \mathbf{k} \cdot \mathbf{c} P \delta\chi_{\mathbf{k}}, \quad (58)$$

where we have used that

$$P_\perp \Lambda P = 0, \quad (59)$$

which is obtained straightforwardly since ξ_β are right eigenfunctions of Λ . We note, however, that the $\{\bar{\xi}_\beta\}_{\beta=1,\dots,3}$ are not left eigenfunctions of Λ , so that $P \Lambda P_\perp \neq 0$. This also means that P and Λ do not commute.

Equations (57) and (58) for the functions $P \delta\chi_{\mathbf{k}}$ and $P_\perp \delta\chi_{\mathbf{k}}$ are coupled. Nevertheless, we shall see that, under certain conditions, we can decouple the equation for $P \delta\chi_{\mathbf{k}}$. If we solve Eq. (58) formally, we obtain

$$P_\perp \delta\chi_{\mathbf{k}}(\mathbf{c}, \tau) = G_0(\tau) P_\perp \delta\chi_{\mathbf{k}}(\mathbf{c}, 0) - \int_0^\tau d\tau' G_{\tau'}(\tau - \tau') \times P_\perp il_H(\tau') \mathbf{k} \cdot \mathbf{c} P \delta\chi_{\mathbf{k}}(\mathbf{c}, \tau'), \quad (60)$$

where we have introduced the operator $G_{\tau'}(\tau - \tau')$ defined from

$$\frac{d}{d\tau} G_{\tau'}(\tau - \tau') = P_\perp [\Lambda(\mathbf{c}) - il_H(\tau) \mathbf{k} \cdot \mathbf{c}] P_\perp G_{\tau'}(\tau - \tau'), \quad G_{\tau'}(0) = 1. \quad (61)$$

Restricting the initial condition to the hydrodynamic subspace, i.e., $P_\perp \delta\chi_{\mathbf{k}} = 0$, we can decouple the equation for $P \delta\chi_{\mathbf{k}}$. If we substitute in Eq. (60) this initial condition, we obtain

$$P_\perp \delta\chi_{\mathbf{k}}(\mathbf{c}, \tau) = - \int_0^\tau d\tau' G_{\tau'}(\tau - \tau') P_\perp il_H(\tau - \tau') \times \mathbf{k} \cdot \mathbf{c} P \delta\chi_{\mathbf{k}}(\mathbf{c}, \tau - \tau'), \quad (62)$$

and we see, by substituting Eq. (62) in (57), that we obtain an involved but closed equation for $P \delta\chi_{\mathbf{k}}$.

The set of hydrodynamic equations (31)–(33) have been obtained through the projection of the Boltzmann equation onto the hydrodynamic subspace. It now appears that the use of Eq. (62) will allow us to close these equations by substituting

tuting the distribution function by its decomposition in terms of the projectors, $\delta\chi_{\mathbf{k}} = P\delta\chi_{\mathbf{k}} + P_{\perp}\delta\chi_{\mathbf{k}}$. This is the aim of the next section.

IV. LINEAR HYDRODYNAMIC EQUATIONS IN NAVIER-STOKES ORDER

In this section we shall use the decomposition of $\delta\chi_{\mathbf{k}}$ into its hydrodynamic part, $P\delta\chi_{\mathbf{k}}$, and nonhydrodynamic part, $P_{\perp}\delta\chi_{\mathbf{k}}$, to close the linear hydrodynamic equations (31)–(33). We shall do so in Navier-Stokes order, that is, in the long-time limit and in second order in the gradients (order k^2).

Let us first introduce $P\delta\chi_{\mathbf{k}}$ in the linear pressure tensor and in the heat flux vector. Here the calculation is straightforward and we obtain

$$\Pi[P\delta\chi_{\mathbf{k}}] = \mathbf{0}, \quad \phi[P\delta\chi_{\mathbf{k}}] = \mathbf{0}, \quad (63)$$

because the functions $\chi_H(\mathbf{c})\Delta(\mathbf{c})$ and $\chi_H(\mathbf{c})\Sigma(\mathbf{c})$ are orthogonal to the subspace spanned by the hydrodynamic eigenfunctions $\{\xi_{\beta}(\mathbf{c})\}_{\beta=1,\dots,3}$. Turning our attention to the other functionals $\delta\zeta_n$, $\delta\zeta_u$, and $\delta\zeta_T$, the calculations become somewhat lengthy, and we show the details in Appendix D. We obtain

$$\delta\zeta_n[P\delta\chi_{\mathbf{k}}] = -4\zeta_n\rho_{\mathbf{k}} - \zeta_n\theta_{\mathbf{k}}, \quad (64)$$

$$\delta\zeta_u[P\delta\chi_{\mathbf{k}}] = -2\zeta_u\mathbf{w}_{\mathbf{k}}, \quad (65)$$

$$\delta\zeta_T[P\delta\chi_{\mathbf{k}}] = -4\zeta_T\rho_{\mathbf{k}} - (3\zeta_T + 2\zeta_n)\theta_{\mathbf{k}}. \quad (66)$$

The negative signs occurring on the right-hand side of these relations account for the fact that a fluctuation with a local enhanced density will induce an increased collision rate, and hence a faster density decay. The same remark holds for temperature or local velocity flow fluctuations.

We now have to calculate the contribution of $P_{\perp}\delta\chi_{\mathbf{k}}$ to the same functionals, to second order in k . This requires the knowledge of $P_{\perp}\delta\chi_{\mathbf{k}}$ to first order in k since the heat flux and pressure tensor enter the balance Eqs. (31)–(33) through their gradients and are already weighted by a factor k . However, it should be noted that, for consistency, the decay rates should be computed to second order in the gradients [see Eqs. (31)–(33)]. We shall nevertheless restrict ourselves to first order, henceforth neglecting the various terms of order 2 that symmetry allows (such as $\nabla^2 n$ and $\nabla^2 T$ for $\delta\zeta_n$ and $\delta\zeta_T$, or $\nabla^2 \mathbf{u}$ for $\delta\zeta_u$). We will comment further on this approximation below. To leading order, we have that $G_{\tau-\tau'}(\tau') \approx e^{P_{\perp}\Lambda P_{\perp}\tau'}$, so that we obtain from Eq. (62)

$$\begin{aligned} P_{\perp}\delta\chi_{\mathbf{k}}(\mathbf{c}, \tau) &\approx - \int_0^{\tau} d\tau' e^{P_{\perp}\Lambda P_{\perp}\tau'} P_{\perp} i l_H(\tau - \tau') \mathbf{k} \cdot \mathbf{c} P \delta\chi_{\mathbf{k}}(\mathbf{c}, \tau - \tau') \\ &\approx - l_H(\tau) \int_0^{\tau} d\tau' e^{P_{\perp}\Lambda P_{\perp}\tau'} e^{-2p\zeta_n\tau'} P_{\perp} i \mathbf{k} \cdot \mathbf{c} P \delta\chi_{\mathbf{k}}(\mathbf{c}, \tau - \tau'), \end{aligned} \quad (67)$$

where we have used that $l_H(\tau) \propto e^{2p\zeta_n\tau}$ [Eq. (27)]. We now have to relate $P\delta\chi_{\mathbf{k}}(\tau - \tau')$ to $P\delta\chi_{\mathbf{k}}(\tau)$, and to be consistent

with the approximation made above, we also have to restrict ourselves to leading order in k . In doing so, Markovian equations for the fields will be derived. From Eq. (57), we get

$$\begin{aligned} P\delta\chi_{\mathbf{k}}(\mathbf{c}, \tau - \tau') &\approx e^{-P\Lambda P\tau'} P\delta\chi_{\mathbf{k}}(\mathbf{c}, \tau) \\ &= \sum_{\beta=1}^3 e^{-\lambda_{\beta}\tau'} \langle \bar{\xi}_{\beta} | \delta\chi_{\mathbf{k}}(\tau) \rangle \xi_{\beta}(\mathbf{c}). \end{aligned} \quad (68)$$

Substituting (68) in (67), we obtain an equation for $P_{\perp}\delta\chi_{\mathbf{k}}$ to first order in k ,

$$\begin{aligned} P_{\perp}\delta\chi_{\mathbf{k}}^{(1)}(\mathbf{c}, \tau) &= - l_H(\tau) \sum_{\beta=1}^3 \langle \bar{\xi}_{\beta} | \delta\chi_{\mathbf{k}}(\tau) \rangle \\ &\quad \times \int_0^{\tau} d\tau' e^{P_{\perp}(\Lambda - 2p\zeta_n - \lambda_{\beta})P_{\perp}\tau'} P_{\perp} i \mathbf{k} \cdot \mathbf{c} \xi_{\beta}(\mathbf{c}), \end{aligned} \quad (69)$$

where $P_{\perp}\delta\chi_{\mathbf{k}} = P_{\perp}\delta\chi_{\mathbf{k}}^{(1)} + O(k^2)$. The pressure tensor and the heat flux up to first order in the gradients of the fields are now obtained by substituting Eq. (69) into Eqs. (34) and (35). Taking into account the symmetry properties of the system, the resulting expressions can be written in the form

$$\Pi_{ij}[P_{\perp}\delta\chi_{\mathbf{k}}^{(1)}] = - i l_H(\tau) \tilde{\eta}(\tau) \left(k_j w_{i,\mathbf{k}} + k_i w_{j,\mathbf{k}} + \frac{2}{d} \mathbf{k} \cdot \mathbf{w}_{\mathbf{k}} \delta_{ij} \right), \quad (70)$$

$$\phi[P_{\perp}\delta\chi_{\mathbf{k}}^{(1)}] = - i l_H(\tau) \mathbf{k} [\bar{\kappa}(\tau) \theta_{\mathbf{k}} + \bar{\mu}(\tau) \rho_{\mathbf{k}}]. \quad (71)$$

Equation (70) is the expected Navier-Stokes expression for the pressure tensor, involving the shear viscosity coefficient $\tilde{\eta}$, but Eq. (71) contains, besides the usual Fourier law characterized by the heat conductivity $\bar{\kappa}$, an additional contribution proportional to the density gradient and with an associated transport coefficient $\bar{\mu}$. This latter term is analogous to the one appearing in granular gases [3,19].

The expressions of the (time-dependent) transport coefficients are

$$\begin{aligned} \tilde{\eta}(\tau) &= \int d\mathbf{c} \Delta_{xy}(\mathbf{c}) F_{3,xy}(\mathbf{c}, \tau) \\ &= \frac{1}{d^2 + d - 2} \sum_{ij}^d \int d\mathbf{c} \Delta_{ij}(\mathbf{c}) F_{3,ij}(\mathbf{c}, \tau), \end{aligned} \quad (72)$$

$$\bar{\mu}(\tau) = \frac{1}{d(1+z)} \int d\mathbf{c} \Sigma(\mathbf{c}) [\mathbf{F}_1(\mathbf{c}, \tau) + \mathbf{F}_2(\mathbf{c}, \tau)], \quad (73)$$

$$\bar{\kappa}(\tau) = \frac{1}{2d(1+z)} \int d\mathbf{c} \Sigma(\mathbf{c}) [-z\mathbf{F}_1(\mathbf{c}, \tau) + \mathbf{F}_2(\mathbf{c}, \tau)], \quad (74)$$

where we have introduced the functions

$$F_{3,ij}(\mathbf{c}, \tau) = \int_0^{\tau} d\tau' e^{P_{\perp}(\Lambda - 2p\zeta_n - p\zeta_T)\tau'} P_{\perp} c_i \xi_{3,j}(\mathbf{c}), \quad (75)$$

$$\mathbf{F}_1(\mathbf{c}, \tau) = \int_0^\tau d\tau' e^{P_\perp(\Lambda - 2p\zeta_n)\tau'} P_\perp \mathbf{c} \xi_1(\mathbf{c}), \quad (76)$$

$$\mathbf{F}_2(\mathbf{c}, \tau) = \int_0^\tau d\tau' e^{P_\perp(\Lambda - p\zeta_T)\tau'} P_\perp \mathbf{c} \xi_2(\mathbf{c}), \quad (77)$$

and in the second equality of Eq. (72) we have summed over all the i, j , taking into account the symmetry of the linearized Boltzmann operator.

Similarly, we calculate the deviations of the decay rates to first order in the gradients of the fields by substituting Eq. (69) into Eqs. (38)–(40). Taking into account the symmetry properties, we arrive at

$$\delta\zeta_n[P_\perp \delta\chi_k^{(1)}] = 0, \quad (78)$$

$$\delta\zeta_u[P_\perp \delta\chi_k^{(1)}] = i l_H(\tau) \mathbf{k} [\zeta_{u,\rho}(\tau) \rho_{\mathbf{k}} + \zeta_{u,\theta}(\tau) \theta_{\mathbf{k}}], \quad (79)$$

$$\delta\zeta_T[P_\perp \delta\chi_k^{(1)}] = 0. \quad (80)$$

The expressions for the coefficients are

$$\begin{aligned} \zeta_{u,\rho}(\tau) &= \frac{\gamma\beta}{d(1+z)} \int d\mathbf{c}_1 \int d\mathbf{c}_2 \chi_H(\mathbf{c}_1) c_{12}(\mathbf{c}_1 + \mathbf{c}_2) \\ &\quad \cdot [\mathbf{F}_1(\mathbf{c}_2, \tau) + \mathbf{F}_2(\mathbf{c}_2, \tau)], \end{aligned} \quad (81)$$

$$\begin{aligned} \zeta_{u,\theta}(\tau) &= \frac{\gamma\beta}{2d(1+z)} \int d\mathbf{c}_1 \int d\mathbf{c}_2 \chi_H(\mathbf{c}_1) c_{12}(\mathbf{c}_1 + \mathbf{c}_2) \\ &\quad \cdot [-z\mathbf{F}_1(\mathbf{c}_2, \tau) + \mathbf{F}_2(\mathbf{c}_2, \tau)], \end{aligned} \quad (82)$$

with $\beta = \pi^{(d-1)/2} / \Gamma[(d+1)/2]$ the d -dimensional solid angle.

At this point, it is important to note that the transport coefficients defined in Eqs. (72)–(74), (81), and (82) are time dependent, and this dependence is governed by the \mathbf{F}_i functions. The (exponential) integrands appearing in the definitions of the \mathbf{F}_i decay with the nonhydrodynamic (kinetic) modes, as a consequence of the action of the projector P_\perp . If we assume that all kinetic eigenvalues are smaller than the smallest hydrodynamic eigenvalue of Λ , which is $\lambda_2 = -p\zeta_T - 2p\zeta_n$, i.e., we assume that there is scale separation, the integrals (75)–(77) converge for $\tau \rightarrow \infty$. It is worth pointing out that we have not proved scale separation, but we will assume it in the following. For an explicit discussion of the scale separation assumption in a similar but somewhat simplified context, we refer to Appendix C, already alluded to above. In order for the transport coefficients to reach their $\tau \rightarrow \infty$ limit faster than any of the hydrodynamic time scales, we need moreover the more stringent condition that the fastest kinetic mode is at least separated by a $p\zeta_T$ gap from $\lambda_2 = -p\zeta_T - 2p\zeta_n$: under this condition, the time dependence of the exponential term in the integral giving \mathbf{F}_2 is fast enough so that the transport coefficients, which depend on the \mathbf{F}_i functions through (72)–(74), can be considered as constants on the hydrodynamic time scale. With this proviso in mind, it is possible to set $\tau \rightarrow \infty$ in the integrals (75)–(77) and the time-independent transport coefficients obtained in this section are then equivalent to those calculated in Ref. [13] by the Chapman-Enskog method. We recall in Appendix A their

expressions in the first-order Sonine approximation. Note that the meaning of the limit $\tau \rightarrow \infty$ in the transport coefficients is $\tau \gg \tau_K$, where τ_K is the typical kinetic scale. This limit can be taken essentially due to the hypothesis of time scale separation.

Finally, if we substitute the expressions derived above for the fluxes, Eqs. (70) and (71), and the decay rates, Eqs. (78)–(80), and we take into account that in the hydrodynamic time scale we can substitute all the coefficients by their values in the $\tau \rightarrow \infty$ limit, we obtain the following closed equations for the linear deviation of the hydrodynamic fields:

$$\left(\frac{\partial}{\partial \tau} + 2p\zeta_n \right) \rho_{\mathbf{k}} + i l_H(\tau) k w_{\mathbf{k}\parallel} + p\zeta_n \theta_{\mathbf{k}} = 0, \quad (83)$$

$$\left(\frac{\partial}{\partial \tau} - p\zeta_T + l_H^2(\tau) \tilde{\eta} k^2 \right) \mathbf{w}_{\mathbf{k}\perp} = \mathbf{0}, \quad (84)$$

$$\begin{aligned} \left(\frac{\partial}{\partial \tau} - p\zeta_T + \frac{2(d-1)}{d} l_H^2(\tau) \tilde{\eta} k^2 \right) w_{\mathbf{k}\parallel} + \frac{i}{2} l_H(\tau) \\ \times k [(1 - 2p\zeta_{u,\rho}) \rho_{\mathbf{k}} + (1 - 2p\zeta_{u,\theta}) \theta_{\mathbf{k}}] = 0, \end{aligned} \quad (85)$$

$$\begin{aligned} \left(\frac{\partial}{\partial \tau} + p\zeta_T + \frac{2}{d} l_H^2(\tau) \tilde{\kappa} k^2 \right) \theta_{\mathbf{k}} + \left(2p\zeta_T + \frac{2}{d} l_H^2(\tau) \tilde{\mu} k^2 \right) \rho_{\mathbf{k}} \\ + i \frac{2}{d} l_H(\tau) k w_{\mathbf{k}\parallel} = 0, \end{aligned} \quad (86)$$

where $w_{\mathbf{k}\parallel}$ and $\mathbf{w}_{\mathbf{k}\perp}$ are the longitudinal and transverse parts of the velocity vector defined by

$$w_{\mathbf{k}\parallel} = \mathbf{w}_{\mathbf{k}} \cdot \hat{\mathbf{k}}, \quad \mathbf{w}_{\mathbf{k}\perp} = \mathbf{w}_{\mathbf{k}} - w_{\mathbf{k}\parallel} \hat{\mathbf{k}}, \quad (87)$$

and $\hat{\mathbf{k}}$ is the unit vector along the direction given by \mathbf{k} .

Equation (84) for the shear mode is decoupled from the other equations and can be readily integrated. If we introduce a nondimensional wave number $\tilde{k} = l_H(0)k$, scaled by the mean free path at the time origin, we obtain the explicit solution

$$\mathbf{w}_{\mathbf{k}\perp}(\tau) = \exp\left(p\zeta_T \tau - \frac{\tilde{\eta} \tilde{k}^2}{4p\zeta_n} (e^{4p\zeta_n \tau} - 1) \right) \mathbf{w}_{\mathbf{k}\perp}(0). \quad (88)$$

Interestingly, depending on \tilde{k} , the perturbation may initially increase if $p\zeta_T - \tilde{\eta} \tilde{k}^2 > 0$. For long times, however, the exponential $e^{4p\zeta_n \tau}$ always dominates the linear term $p\zeta_T \tau$ and the perturbation decays.

The other three fields, namely, the density $\rho_{\mathbf{k}}$, temperature $\theta_{\mathbf{k}}$, and longitudinal velocity $w_{\mathbf{k}\parallel}$, obey the system of coupled linear equations

$$\frac{\partial}{\partial \tau} \begin{pmatrix} \rho_{\mathbf{k}} \\ w_{\mathbf{k}\parallel} \\ \theta_{\mathbf{k}} \end{pmatrix} = \mathbf{M}(\tau) \cdot \begin{pmatrix} \rho_{\mathbf{k}} \\ w_{\mathbf{k}\parallel} \\ \theta_{\mathbf{k}} \end{pmatrix}, \quad (89)$$

where the time-dependent matrix is

$$\mathbf{M}(\tau) = \begin{pmatrix} -2p\zeta_n & -il_H(\tau)k & -p\zeta_n \\ -\frac{i}{2}l_H(\tau)k(1-2p\zeta_{u,\rho}) & p\zeta_T - \frac{2(d-1)}{d}l_H^2(\tau)\tilde{\eta}k^2 & -\frac{i}{2}l_H(\tau)k(1-2p\zeta_{u,\theta}) \\ -2p\zeta_T - \frac{2}{d}l_H^2(\tau)\tilde{\mu}k^2 & -i\frac{2}{d}l_H(\tau)k & -p\zeta_T - \frac{2}{d}l_H^2(\tau)\tilde{\kappa}k^2 \end{pmatrix}. \quad (90)$$

We note here that this matrix differs from Eq. (59) of Ref. [13], where the analysis amounts to overlooking the time dependence of the mean free path, so that all entries of the hydrodynamic matrix exhibit the same time dependence. The different time dependences present in Eq. (90) render the stability analysis more difficult. For long times, however, the eigenvalues of the matrix $\mathbf{M}(\tau)$ are always negative and the perturbations *a priori* decay. A caveat is nevertheless in order. It is worth pointing out that Eqs. (88) and (89) break down at long times. Indeed, once the function $l_H(\tau)k$ exceeds unity, the expansion in the gradients we have performed is no longer valid, and it would be necessary to include terms of higher order in k . In addition, if the perturbation initially increases sufficiently to leave the linear regime, our description breaks down and it becomes necessary to consider non-linear terms.

Although quite involved, the evolution equations (89) can be numerically integrated, using, for instance, the transport coefficients computed in the Sonine approximation in Appendix A. This is what we do in the next section, in order to compare the theoretical predictions with molecular dynamics simulations.

V. MOLECULAR DYNAMICS SIMULATIONS

To put our theoretical predictions to the test, we have performed molecular dynamics (MD) simulations of a system of N smooth hard disks ($d=2$) which undergo ballistic flights punctuated by collisional events: at each collision, the disks annihilate with probability p ; otherwise, they collide elastically. The particles are localized in a square box of size L with periodic boundary conditions. An event-driven algorithm [20] has been used and the initial density has been chosen low enough to be always in the dilute limit. The parameters for all the MD simulations are $N(0)=10^5$ and reduced density $n(0)\sigma^2=0.05$ where σ is the disk radius and $0 < p \leq 1$. The initial conditions we have considered correspond to small-amplitude perturbations around the homogeneous decay state, to enforce the validity of the linearized hydrodynamic equations (83)–(86).

A. Perturbation of the transverse velocity

Since Eq. (84) for the shear mode is decoupled from the other equations, one of the simplest macroscopic perturbations one can think of consists in an initial harmonic perturbation of the transverse component of the velocity field,

whose evolution is given by Eq. (88). We shall consider a small perturbation in real space of the form

$$u_x(\mathbf{r}, 0) = A \sin(k_m y), \quad (91)$$

with $A=10^{-1}v_H(0)$ and $k_m=2\pi/L$, where L is the linear size of the system. The reason for choosing the smallest possible value of k compatible with the boundary conditions is two-fold. First, the corresponding mode is the most unstable at short times [see Eq. (88)]. For the parameters of the simulations, we indeed probe the region where $p\zeta_T > \tilde{\eta}k^2$, so that the hydrodynamic equation (88) predicts an initial *increase* of the perturbation. Second, the low- k regime is that where our large-scale predictions are most likely to be relevant.

Figure 1 displays the evolution of $w_{k_m\perp}$ as a function of the number of collisions per particle τ for a system with $p=0.1$, averaging data over 50 different trajectories. The solid line is the simulation result and the dashed line is the theoretical prediction Eq. (88), where the shear viscosity and the decay rates have been computed using the standard tools of kinetic theory (here, the first Sonine approximation [13], see Appendix A). An excellent agreement is obtained *without any adjustable parameter*, including the predicted increase of the perturbation at short times, and as also observed for a larger annihilation probability $p=0.5$ (see Fig. 2, in which the MD data are obtained by an average over 150 runs).

Recalling that $n_H(\tau)/n_H(0)=\exp(-2p\zeta_n\tau)$ and that $v_H(\tau)=v_H(0)\exp(-p\zeta_T\tau)$, it proves also convenient to consider the actual velocity field $\delta\mathbf{u}(\tau)=v_H(\tau)\mathbf{w}(\tau)$ instead of its dimensionless counterpart \mathbf{w} , since the prediction (88) then takes the form

$$\delta u_{\mathbf{k}\perp}(\tau) = \exp\left[-\frac{\tilde{\eta}k^2}{4p\zeta_n}\left(\frac{n_H^2(0)}{n_H^2(\tau)} - 1\right)\right] \delta u_{\mathbf{k}\perp}(0). \quad (92)$$

The plot of $\delta u_{\mathbf{k}\perp}(\tau)/\delta u_{\mathbf{k}\perp}(0)$ as a function of $[n_H(0)/n_H(\tau)]^2$ allows us then by simple exponential fitting to extract $\tilde{\eta}/\zeta_n$ [recall that $\tilde{k}=l_H(0)k$ is known]. Figure 3 compares the ratios $\tilde{\eta}/\zeta_n$ extracted from such fits for various values of p with the theoretical prediction. We have plotted the value of the viscosity normalized by its elastic value $\tilde{\eta}_e$. For $p=0.1$ the agreement is quite good but for $p=1$ we obtain discrepancies of the order of 15%. Note that in the inelastic case the agreement is better for all values of the inelasticity when the shear viscosity is measured by the direct Monte Carlo simulation method [21]. Such deviations could be due to the limitation

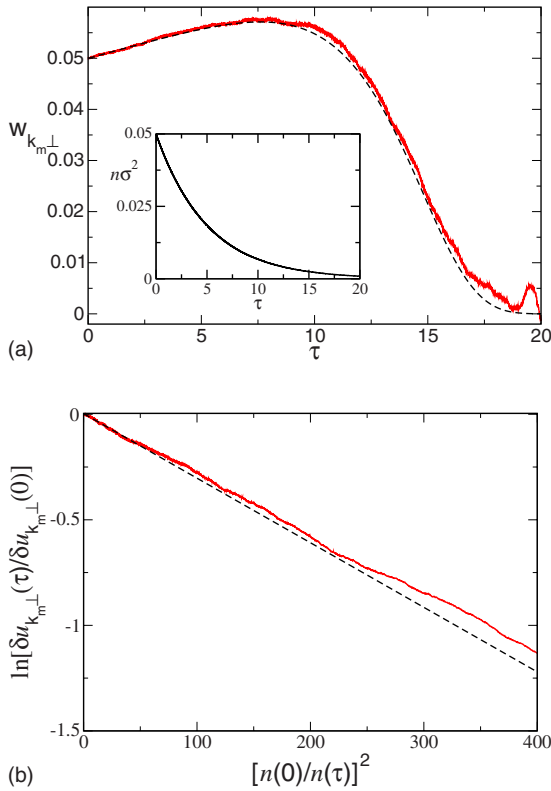


FIG. 1. (Color online) (a) Time evolution of a linear perturbation of the transverse velocity for a system with annihilation probability $p=0.1$. The solid lines are the molecular dynamics results and the dashed lines are the theoretical predictions (no adjustable parameter). Note how the theoretical predictions correctly account for the increase of the perturbation at short times. The inset shows the evolution of density with rescaled time τ , where σ is the disk radius. For $\tau=20$, $n\sigma^2 \approx 9 \times 10^{-4}$. (b) Evolution of $\delta u_{k_{\perp}}(\tau)/\delta u_{k_{\perp}}(0)$ as a function of $n^2(0)/n^2(\tau)$. The dashed line is the exponential decay predicted by Eq. (92). $n^2(0)/n^2(\tau)=400$ corresponds to $\tau \approx 15$.

for high dissipation of the first Sonine approximation that has been used to compute the numerical values of the various quantities involved in the description (in particular, the deviations of the homogeneous decay state velocity distribution from its Gaussian form might be relevant). Additionally, the shear viscosity could suffer from finite-size effects. For a related discussion in the realm of granular gases, where both effects alluded to are at work; see [22–24]. Finally, neglecting the k^2 contribution to $\delta \zeta_{\mathbf{u}}$ might not be innocuous. From symmetry considerations, such a term must be of the form $k^2 l_H(\tau)^2 \mathbf{w}_{\mathbf{k}}$, so that Eq. (84) for the transverse velocity has the same form as the one we considered, but with a “shifted” shear viscosity. It is worth pointing out here that, in the corresponding Eq. (88), putative order- k^2 corrections to $\delta \zeta_n$ and $\delta \zeta_T$ play no role [see Eq. (84)]: the decay rates ζ_n and ζ_T appearing in (88) are fingerprints of the τ dependence of l_H and of the rescaling procedure leading to $\mathbf{w}_{\mathbf{k}}$ from the actual velocity flow. Those two decay rates are therefore properties of the homogeneous solution and do not suffer any finite- k correction.

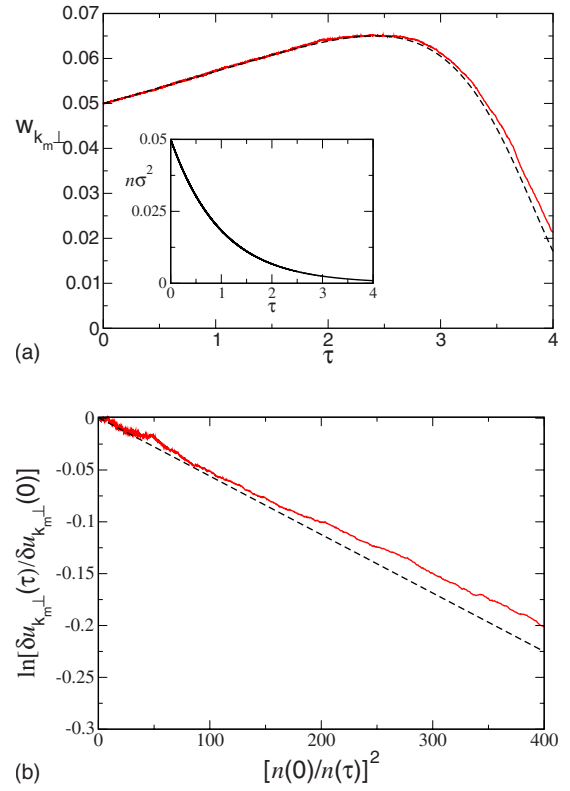


FIG. 2. (Color online) (a) Same as in Fig. 1 but for a system with $p=0.5$, which—loosely speaking—may therefore be considered as being more “distant” from equilibrium. The inset shows the evolution of density with rescaled time τ . For $\tau=4$, the rescaled density is $n\sigma^2 \approx 9 \times 10^{-4}$ [while $n(0)\sigma^2=0.05$]. (b) Evolution of $\delta u_{k_{\perp}}(\tau)/\delta u_{k_{\perp}}(0)$ as a function of $n^2(0)/n^2(\tau)$. $n^2(0)/n^2(\tau)=400$ corresponds to $\tau \approx 3$.

B. Perturbation of the longitudinal velocity

In order to investigate further the validity of the hydrodynamic equations, we consider a perturbation of the longitudinal velocity

$$u_x(\mathbf{r}, 0) = A \sin(k_m x), \quad (93)$$

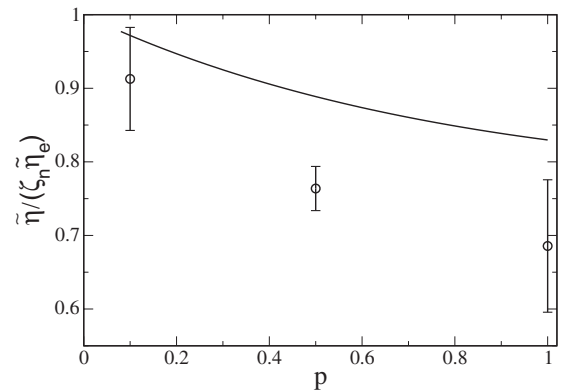


FIG. 3. Symbols: ratio $\tilde{\eta}/\zeta_n$ (normalized by its $p \rightarrow 0$ value) extracted from the exponential fit of $\delta u_{k_{\perp}}(\tau)$ to Eq. (92). The solid line is the theoretical prediction in the first Sonine approximation.

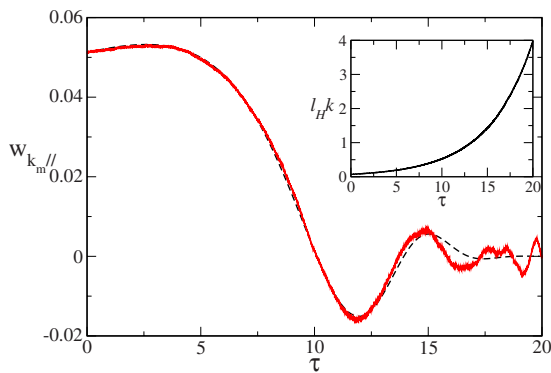


FIG. 4. (Color online) Time evolution of the longitudinal velocity for a system with $p=0.1$ as a function of τ . The solid line shows the simulation results and the dashed line is the numerical solution of (89). For $\tau=15$ the rescaled density is $n\sigma^2 \approx 2.5 \times 10^{-3}$. The inset shows the increase of mean free path with time and that, for $\tau > 10$, $l_H k$ is no longer a small quantity.

where $A = 10^{-1} v_H(0)$ and $k_m = 2\pi/L$. Since the hydrodynamic matrix M depends on time and $\frac{dM}{dt}$ does not commute with M , we could not solve analytically the set of Eqs. (89), and we turned to a numerical integration, using the transport coefficients computed in Appendix A.

In Fig. 4, we have plotted the time evolution of the rescaled longitudinal velocity field $w_{k_m //}$ as a function of the internal time clock τ (number of collisions per particle) for a system with $p=0.1$. The results have been averaged over 16 trajectories. It can be seen that the theoretical framework is able to account for the nontrivial time dependence of the perturbation dynamics. Moreover, as the equations for θ_{k_m} and ρ_{k_m} are coupled with the equation for $w_{k_m //}$, a perturbation such as (93) induces a response of the above two other fields (at variance with the transverse velocity, whose dynamics is decoupled from the other three modes, at least at the linear level of description adopted here). In Fig. 5, we have plotted the energy density $e_{k_m} = \theta_{k_m} + \rho_{k_m}$ and ρ_{k_m} as a function of τ . The agreement with theory is very good both qualitatively and quantitatively, with an evolution that is well predicted up to $\tau \approx 15$; for long times the simulation data become somewhat noisy (less statistics can be achieved due to the smaller

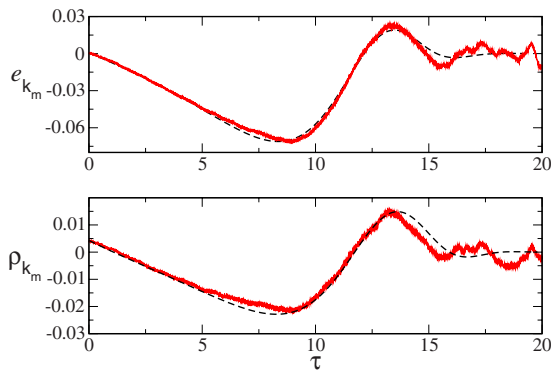


FIG. 5. (Color online) Time evolution of e_{k_m} and ρ_{k_m} as a function of τ for a system with $p=0.1$. The solid lines show molecular dynamics results while the dashed lines are for the numerical solution of (89). For $\tau=15$ the rescaled density is $n\sigma^2 \approx 2.5 \times 10^{-3}$.

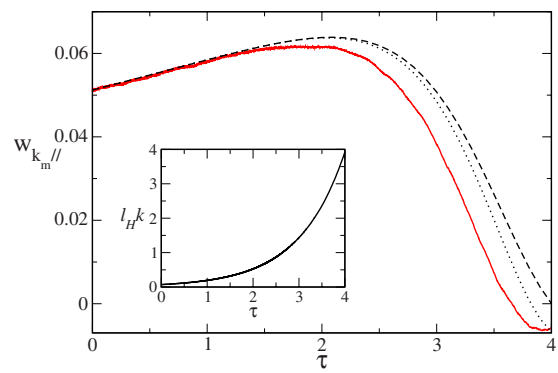


FIG. 6. (Color online) Time evolution of the longitudinal velocity for a system with $p=0.5$ as a function of τ . The solid line shows the simulation results and the dashed line is for the numerical solution. We have also plotted with a dotted line the numerical solution considering the elastic values of $\tilde{\kappa}$ and $\tilde{\mu}$ (i.e., their limit when $p \rightarrow 0^+$). The inset shows the increase of mean free path with time.

number of particles left in the system. The number of particles at $\tau=15$ is $N \approx 5000$).

In Figs. 6 and 7, results for a system with $p=0.5$ are shown. Data are averaged over 64 runs. In this case, the agreement is still good qualitatively, with similar shapes for the theoretical and numerical curves, but some discrepancies are observed. The most significant deviation from the theoretical prediction occurs for the density ρ_{k_m} , where the value of the minimum and also its position are not predicted accurately. However, the hydrodynamic framework still captures correctly the trends of the complex dynamics of the perturbations. The above discrepancies could be ascribable to the failure of the first Sonine approximation for high dissipation (i.e., “high” p) or to finite-size effects. We mention here that within the first Sonine approximation, the dimensionless coefficients $\tilde{\mu}$ and $\tilde{\kappa}$ exhibit a divergent behavior in the vicinity of $p=0.8$ [13], which is presumably unphysical, and is an indication of the limitation of the method. For completeness and to assess the robustness of the predictions with respect to a modification of the numerical values of the key parameters, we have also reported in Figs. 6 and 7 the predictions obtained when the transport coefficients take their elastic hard disk value [e.g., $\tilde{\mu}(p=0.5) \approx 0.505$ while $\tilde{\mu}(p=0)=0$, as re-

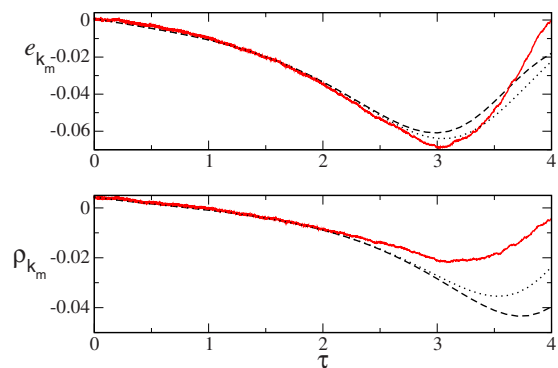


FIG. 7. (Color online) Time evolution of e_{k_m} and ρ_{k_m} as a function of τ for a system with $p=0.5$. The different lines have the same meaning as in Fig. 6.

quired by Fourier's law]. The important point is that the time evolutions are not significantly affected, and that the main features remain the same. Additionally, as mentioned after Eqs. (66) and (92), a possible source of inaccuracy lies in the truncation of decay rates to their first order (k^1) in the gradients. While the corresponding terms have been shown to be small for inelastic hard spheres [25] (with the notable simplification there that the velocity decay rate vanishes identically due to momentum conservation), their relevance in the present case has not been assessed, apart from indirectly for the velocity decay rate $\delta\zeta_u$, by noting that second-order corrections do not spoil the accuracy of the prediction (88); see Figs. 1 and 2.

VI. CONCLUSIONS

The objective here has been to explore the validity of a hydrodynamic description based on density, momentum, and kinetic temperature fields for a gas composed of particles which annihilate with probability p or scatter elastically otherwise, by a direct analysis of the spectrum of the linear Boltzmann equation. The motivation mainly was to study the applicability of hydrodynamics to systems where scale separation is not granted *a priori* and in which there are no collisional invariants. The analysis performed here has been shown to lead to results equivalent to those obtained previously from the more formal Chapman-Enskog expansion [13], with the difference that the present approach considers linear excitations only. However, the current spectral method is arguably more straightforward and explicitly shows that the hydrodynamic description arises in the appropriate time scale, when the kinetic modes can be considered as negligible compared to the hydrodynamic ones.

The eigenvalue problem of the Boltzmann operator linearized around the homogeneous decay state has been addressed and we have identified the hydrodynamic eigenfunctions. These eigenfunctions are not simply linear combinations of 1 , \mathbf{v} , and v^2 as in the elastic case, but they are replaced by derivatives of the homogeneous decay state velocity distribution function χ_H , which is not known analytically. As a consequence of the non-Hermitian character of the linearized Boltzmann operator, the eigenfunctions are not orthogonal. It is nevertheless possible to construct a set of biorthonormal functions $\{\bar{\xi}_\beta\}_{\beta=1,\dots,3}$, which are linear combinations of 1 , \mathbf{v} , and v^2 , a crucial point in order to obtain the hydrodynamic equations. The analysis is complicated by the fact that none of the $\{\bar{\xi}_\beta\}$ functions are left eigenfunctions of the linearized Boltzmann operator, since no quantity is conserved during binary encounters. We have used these hydrodynamic eigenfunctions to derive to Navier-Stokes order the heat and momentum fluxes, together with the various decay rates. To this end, we have decomposed the distribution function $\delta\chi_{\mathbf{k}}$ into its hydrodynamic and nonhydrodynamic parts. This decomposition enables us to close the hydrodynamic equations in the long-time limit and to order k^2 , and provides Green-Kubo formulas for the transport coefficients. We then arrived at the linearized equations (around the homogeneous decay state) for the hydrodynamic fields, in the usual form of partial differential equations with coefficients that are independent of

the space variable but depend on time, since the reference state considered is itself time dependent. If we analyze the stability of these equations, we may conclude that small perturbations should decay in the long-time limit. Nevertheless, it must be stressed that the perturbation may increase at short times, thereby possibly leaving the linear domain where our analysis holds. The long-time dynamics in such a case remains an open question.

In Sec. V, we have reported molecular dynamics simulations for the evolution of a perturbation of the transverse and longitudinal velocity fields, which show a rich dynamics. The agreement between theory and simulations is very good for moderate values of the annihilation probability p (say $p < 0.5$), which gives strong support to the theoretical analysis developed here. The theoretical curves still agree qualitatively at larger p , with, however, some quantitative discrepancies which might be a manifestation of the approximations underlying the computation of the transport coefficients (namely, κ and μ , evaluated to first order in a Sonine expansion [13]). Indeed, those coefficients are predicted to exhibit a divergent behavior for $p \sim 0.8$, but the simulations we have performed do not show a qualitatively different behavior for these values of p . A further complication—that is also an *a priori* limitation for the efficiency of a hydrodynamic approach—is that for values of p close to unity, the separation of time scales between the kinetic and hydrodynamic modes is not clear-cut (the density decay rate is on the order of the collision frequency, comparable to the inverse typical time of the kinetic modes). To address this concern, one should study in detail the spectrum of nonhydrodynamic modes to find the slowest, and compare it to the fastest decay rate in our problem (i.e., ζ_n). Such a program, left for future work, has been achieved in Appendix C within the Maxwell model framework, with the conclusion that scale separation does not hold for $p > p^* = 1/4$. While the threshold p^* is *a priori* model dependent, a similar phenomenon is to be expected in the original “hard-sphere” dynamics considered in this paper. The coarse-grained description for $p > p^*$ is an open question.

ACKNOWLEDGMENTS

We would like to thank the Agence Nationale de la Recherche for financial support (Grant No. ANR-05-JCJC-44482). M.I.G.S. acknowledges financial support from Becas de la Fundación La Caixa y el Gobierno Francés and from the HPC-EUROPA Project No. RII3-CT-2003-506079, with the support of the European Community Research Infrastructure Action. P.M. acknowledges financial support from the Programa José Castillejo of the Spanish Minister of Education and Science.

APPENDIX A: APPROXIMATE EXPRESSION FOR THE TRANSPORT COEFFICIENTS AND DECAY RATES

For completeness, we recall here the explicit expressions used for the transport coefficients and decay rates, as obtained within the first-order Sonine scheme in Ref. [13]. The distribution function in this approximation reads

$$\chi_H(c) = \frac{1}{\pi^{d/2}} e^{-c^2} \left[1 + a_2 \left(\frac{d(d+2)}{8} - \frac{d+2}{2} c^2 + \frac{c^4}{2} \right) \right], \quad (\text{A1})$$

with the kurtosis

$$a_2 = \frac{8(3 - 2\sqrt{2})p}{(4d + 6 - \sqrt{2})p + 8\sqrt{2}(d-1)(1-p)}. \quad (\text{A2})$$

This expression allows us to calculate the decay rates

$$\zeta_n = \frac{d+2}{4} \left(1 - a_2 \frac{1}{16} \right), \quad (\text{A3})$$

$$\zeta_T = \frac{d+2}{8d} \left(1 + a_2 \frac{8d+11}{16} \right), \quad (\text{A4})$$

and also the transport coefficients

$$\tilde{\eta} = \frac{1}{4\nu_\eta - 2p\zeta_T}, \quad (\text{A5})$$

$$\tilde{\kappa} = \frac{1}{\nu_\kappa - 2p\zeta_T} \left(\frac{1}{2} p \zeta_n \tilde{\mu} + \frac{d+2}{8} (2a_2 + 1) \right), \quad (\text{A6})$$

$$\tilde{\mu} = \frac{1}{2\nu_\kappa - 3p\zeta_T - 2p\zeta_n} \left(p\zeta_T \tilde{\kappa} + \frac{d+2}{8} (2a_2 + 1) \right), \quad (\text{A7})$$

where the values of the coefficients ν_η and ν_κ are

$$\nu_\eta = \frac{p}{8d} \left(3 + 6d + 2d^2 - a_2 \frac{278 + 375d + 96d^2 + 2d^3}{32(d+2)} \right) + (1-p) \left(1 - a_2 \frac{1}{32} \right), \quad (\text{A8})$$

$$\nu_\kappa = \frac{p}{32d} \left(16 + 27d + 8d^2 + a_2 \frac{2880 + 1544d - 2658d^2 - 1539d^3 - 200d^4}{32d(d+2)} \right) + (1-p) \frac{d-1}{d} \left(1 + a_2 \frac{1}{32} \right). \quad (\text{A9})$$

Finally, the expressions for $\zeta_{u,p}$ and $\zeta_{u,\theta}$ are

$$\zeta_{u,p} = \frac{8(d-1)}{d(d+2)} \tilde{\mu} \zeta_u, \quad (\text{A10})$$

$$\zeta_{u,\theta} = \frac{8(d-1)}{d(d+2)} \tilde{\kappa} \zeta_u, \quad (\text{A11})$$

with

$$\zeta_u = \frac{(d+2)^2}{32(d-1)} \left(1 + a_2 \frac{-86 - 101d + 32d^2 + 88d^3 + 28d^4}{32(d+2)} \right). \quad (\text{A12})$$

APPENDIX B: EIGENFUNCTIONS OF Λ

In this appendix some of the details leading to the solution of the eigenvalue problem (41) are given. Consider first the function

$$\Psi_1(\mathbf{c}) = \chi_H(\mathbf{c}) \quad (\text{B1})$$

and let the linearized operator Λ act on χ_H ,

$$\begin{aligned} \Lambda(\mathbf{c}_1)\chi_H(\mathbf{c}_1) &= \gamma \int d\mathbf{c}_2 T(\mathbf{c}_1, \mathbf{c}_2) (1 + \mathcal{P}_{12}) \chi_H(\mathbf{c}_1) \chi_H(\mathbf{c}_2) \\ &\quad + p(2\zeta_n - d\zeta_T) \chi_H(\mathbf{c}_1) - p\zeta_T \mathbf{c}_1 \cdot \frac{\partial}{\partial \mathbf{c}_1} \chi_H(\mathbf{c}_1). \end{aligned} \quad (\text{B2})$$

If we take into account the equation for $\chi_H(\mathbf{c}_1)$,

$$\begin{aligned} (d\zeta_T - 2\zeta_n) p \chi_H(\mathbf{c}_1) + p\zeta_T \mathbf{c}_1 \cdot \frac{\partial}{\partial \mathbf{c}_1} \chi_H(\mathbf{c}_1) \\ = \gamma \int d\mathbf{c}_2 T(\mathbf{c}_1, \mathbf{c}_2) \chi_H(\mathbf{c}_1) \chi_H(\mathbf{c}_2), \end{aligned} \quad (\text{B3})$$

we can rewrite Eq. (B2) as

$$\Lambda(\mathbf{c}_1)\chi_H(\mathbf{c}_1) = (d\zeta_T - 2\zeta_n) p \chi_H(\mathbf{c}_1) + p\zeta_T \mathbf{c}_1 \cdot \frac{\partial}{\partial \mathbf{c}_1} \chi_H(\mathbf{c}_1). \quad (\text{B4})$$

Consider now the function

$$\Psi_2(\mathbf{c}) = \mathbf{c} \cdot \frac{\partial}{\partial \mathbf{c}} \chi_H(\mathbf{c}). \quad (\text{B5})$$

In order to proceed, we perform the change of variables $\mathbf{c}_1 = \lambda \mathbf{c}'_1$ in Eq. (B3),

$$\begin{aligned} (d\zeta_T - 2\zeta_n) p \chi_H(\lambda \mathbf{c}'_1) + p\zeta_T \mathbf{c}'_1 \cdot \frac{\partial}{\partial \mathbf{c}'_1} \chi_H(\lambda \mathbf{c}'_1) \\ = \gamma \lambda^{d+1} \int d\mathbf{c}'_2 \int d\hat{\sigma} \theta(\mathbf{c}'_{12} \cdot \hat{\sigma}) \mathbf{c}'_{12} \cdot \hat{\sigma} \\ \times [(1-p)b_\sigma^{-1} - 1] \chi_H(\lambda \mathbf{c}'_1) \chi_H(\lambda \mathbf{c}'_2). \end{aligned} \quad (\text{B6})$$

Taking derivatives with respect to λ , we obtain

$$\begin{aligned} (d\zeta_T - 2\zeta_n) p \frac{\partial}{\partial \lambda} \chi_H(\lambda \mathbf{c}_1) + p\zeta_T \mathbf{c}_1 \cdot \frac{\partial}{\partial \mathbf{c}_1} \left(\frac{\partial}{\partial \lambda} \chi_H(\lambda \mathbf{c}_1) \right) \\ = (d+1) \lambda^d \gamma \int d\mathbf{c}_2 T(\mathbf{c}_1, \mathbf{c}_2) \chi_H(\lambda \mathbf{c}_1) \chi_H(\lambda \mathbf{c}_2) \\ + \gamma \lambda^{d+1} \int d\mathbf{c}_2 T(\mathbf{c}_1, \mathbf{c}_2) \frac{\partial \chi_H(\lambda \mathbf{c}_1)}{\partial \lambda} \chi_H(\lambda \mathbf{c}_2) \\ + \gamma \lambda^{d+1} \int d\mathbf{c}_2 T(\mathbf{c}_1, \mathbf{c}_2) \chi_H(\lambda \mathbf{c}_1) \frac{\partial \chi_H(\lambda \mathbf{c}_2)}{\partial \lambda} \end{aligned} \quad (\text{B7})$$

and taking $\lambda=1$, we arrive at the equation for $\Psi_2(\mathbf{c})$,

$$\begin{aligned}
& (d\zeta_T - 2\zeta_n)p\Psi_2(\mathbf{c}_1) + p\zeta_T\mathbf{c}_1 \cdot \frac{\partial}{\partial\mathbf{c}_1}\Psi_2(\mathbf{c}_1) \\
&= (d+1)\gamma \int d\mathbf{c}_2 T(\mathbf{c}_1, \mathbf{c}_2) \chi_H(\lambda\mathbf{c}_1) \chi_H(\lambda\mathbf{c}_2) \\
&+ \gamma \int d\mathbf{c}_2 T(\mathbf{c}_1, \mathbf{c}_2) \Psi_2(\mathbf{c}_1) \chi_H(\lambda\mathbf{c}_2) \\
&+ \gamma \int d\mathbf{c}_2 T(\mathbf{c}_1, \mathbf{c}_2) \chi_H(\lambda\mathbf{c}_1) \Psi_2(\mathbf{c}_2), \tag{B8}
\end{aligned}$$

or equivalently

$$\begin{aligned}
\Lambda(\mathbf{c}_1)\Psi_2(\mathbf{c}_1) = & -(d+1) \left((d\zeta_T - 2\zeta_n)p\chi_H(\mathbf{c}_1) \right. \\
& \left. + p\zeta_T\mathbf{c}_1 \cdot \frac{\partial}{\partial\mathbf{c}_1}\chi_H(\mathbf{c}_1) \right). \tag{B9}
\end{aligned}$$

Consequently, Eqs. (B4) and (B9) can be written as

$$\Lambda(\mathbf{c}_1)\Psi_1(\mathbf{c}_1) = (d\zeta_T - 2\zeta_n)p\Psi_1(\mathbf{c}_1) + p\zeta_T\Psi_2(\mathbf{c}_1), \tag{B10}$$

$$\Lambda(\mathbf{c}_1)\Psi_2(\mathbf{c}_2) = -(d+1)[(d\zeta_T - 2\zeta_n)p\Psi_1(\mathbf{c}_1) + p\zeta_T\Psi_2(\mathbf{c}_1)]. \tag{B11}$$

With Eqs. (B10) and (B11) we can easily see that

$$\Lambda(\mathbf{c}_1)[(d+1)\Psi_1(\mathbf{c}_1) + \Psi_2(\mathbf{c}_1)] = 0, \tag{B12}$$

so that

$$\xi_1(\mathbf{c}_1) \equiv (d+1)\Psi_1(\mathbf{c}_1) + \Psi_2(\mathbf{c}_1) \tag{B13}$$

is an eigenfunction of the operator $\Lambda(\mathbf{c}_1)$ with eigenvalue $\lambda_1=0$. It is also straightforward to see that

$$\xi_2(\mathbf{c}_1) = (d\zeta_T - 2\zeta_n)p\Psi_1(\mathbf{c}_1) + p\zeta_T\Psi_2(\mathbf{c}_1) \tag{B14}$$

is an eigenfunction of Λ . We obtain that

$$\begin{aligned}
\Lambda(\mathbf{c}_1)\xi_2(\mathbf{c}_1) &= (d\zeta_T - 2\zeta_n)p\Lambda(\mathbf{c}_1)\Psi_1(\mathbf{c}_1) + p\zeta_T\Lambda(\mathbf{c}_1)\Psi_2(\mathbf{c}_1) \\
&= -(\zeta_T + 2\zeta_n)p\xi_2(\mathbf{c}_1), \tag{B15}
\end{aligned}$$

where we have used Eqs. (B10) and (B11). Therefore, we have that $\xi_2(\mathbf{c}_1)$ is an eigenfunction of $\Lambda(\mathbf{c}_1)$ with eigenvalue $\lambda_2 = -(\zeta_T + 2\zeta_n)p$.

Finally, let us consider the last function

$$\Psi_3(\mathbf{c}) = -\frac{\partial}{\partial\mathbf{c}}\chi_H(\mathbf{c}). \tag{B16}$$

Taking the derivative of the equation obeyed by $\chi_H(\mathbf{c}-\mathbf{w})$ with respect to \mathbf{w} and subsequently evaluating the result for $\mathbf{w}=\mathbf{0}$, we obtain

$$\begin{aligned}
& (d\zeta_T - 2\zeta_n)p\Psi_3(\mathbf{c}_1) + p\zeta_T\Psi_3(\mathbf{c}_1) + p\zeta_T\mathbf{c}_1 \cdot \frac{\partial}{\partial\mathbf{c}_1}\Psi_3(\mathbf{c}_1) \\
&= \gamma \int d\mathbf{c}_2 T(\mathbf{c}_1, \mathbf{c}_2) (1 + \mathcal{P}_{12})\Psi_3(\mathbf{c}_1) \chi_H(\mathbf{c}_2), \tag{B17}
\end{aligned}$$

or equivalently

$$\Lambda(\mathbf{c}_1)\Psi_3(\mathbf{c}_1) = p\zeta_T\Psi_3(\mathbf{c}_1). \tag{B18}$$

In other words, $\xi_3(\mathbf{c}_1) \equiv \Psi_3(\mathbf{c}_1)$ is an eigenfunction of $\Lambda(\mathbf{c}_1)$ with eigenvalue $\lambda_3 = p\zeta_T$.

APPENDIX C: LINEARIZED BOLTZMANN OPERATOR FOR MAXWELL MOLECULES

The objective in this appendix is to study the spectrum of the linearized Boltzmann operator for Maxwell molecules with annihilation. It will be shown that for $0 \leq p \leq p^*$, where p^* depends on the specific Maxwell model under consideration, the norms of the hydrodynamic eigenvalues are smaller than the rest of the spectrum.

The main characteristic of Maxwell models is that the differential cross section multiplied by the relative velocity is independent of the relative velocity. We are going to assume that it is also independent of the angle between the two colliding particles. Then, the Boltzmann equation for a system of Maxwell molecules which annihilate in a collision with probability p and collide elastically otherwise (with probability $1-p$) reads

$$\begin{aligned}
& \left(\frac{\partial}{\partial t} + \mathbf{v}_1 \cdot \nabla \right) f(\mathbf{r}, \mathbf{v}_1, t) \\
&= -p\beta\Omega \int d\mathbf{v}_2 f(\mathbf{r}, \mathbf{v}_1, t) f(\mathbf{r}, \mathbf{v}_2, t) + (1-p)\beta \int d\mathbf{v}_2 \\
&\quad \times \int d\hat{\sigma} [b_\sigma^{-1} - 1] f(\mathbf{r}, \mathbf{v}_1, t) f(\mathbf{r}, \mathbf{v}_2, t), \tag{C1}
\end{aligned}$$

where β is a constant representing the microscopic scattering collision frequency, $\Omega = 2\pi^{d/2}/\Gamma(d/2)$ is the d -dimensional solid angle, and the operator b_σ^{-1} is defined in the main text, Eq. (4).

If we consider the homogeneous case, it is straightforward to see that the temperature is a constant in time, $T_H(t) = T_H(0)$, and that the density evolves as

$$n_H(t) = \frac{n_H(0)}{1 + p\zeta_n t}, \tag{C2}$$

with $\zeta_n = \beta\Omega n_H(0)$. Moreover, it was shown in [26] that there is an exact mapping between the homogeneous equation for Maxwell molecules with annihilation (arbitrary p) and the usual elastic Maxwell molecules ($p=0$). If we introduce the time scale

$$s(t) = \int_0^t dt' \frac{n_H(t')}{n_H(0)}, \tag{C3}$$

it can be seen that the distribution function for arbitrary p is

$$f(\mathbf{v}, t) = \frac{n_H(t)}{n_H(0)} f^E[\mathbf{v}, (1-p)s(t)], \tag{C4}$$

where $n_H(t)$ is given by formula (C2), $s(t)$ by (C3), and the function f^E is the distribution function for elastic Maxwell molecules. Note that this relation is also valid for $p=1$ where f^E is frozen in the initial condition.

In the elastic case, every homogeneous distribution tends to relax to a Maxwellian after a transient time. Then, the same is going to happen for arbitrary $p < 1$ because of the mapping. In this sense, we can consider that the state analogous to the homogeneous decay state introduced in the main text for hard particles and that will constitute the appropriate reference will be characterized by the distribution function

$$f_H(\mathbf{v}, t) = \frac{n_H(t)}{v_H^d} \chi_M(v/v_H), \quad (\text{C5})$$

where $v_H = (\frac{2T_H}{m})^{1/2}$ and $\chi_M(v) = 1/\pi^{d/2} e^{-v^2}$ is the Maxwellian distribution. Note that, in the homogeneous decay state, both the density and temperature decay, but in the present case only the density decays. Then, as v_H plays no role, we will consider units with $v_H = 1$ for simplicity.

Let us study now the linear response to an inhomogeneous small perturbation around the reference state as in Sec. II. If we introduce the scaled distribution function

$$\delta\chi(\mathbf{r}, \mathbf{v}, \tau) = \frac{n_H(0)}{n_H(t)} [f(\mathbf{r}, \mathbf{v}, t) - f_H(\mathbf{v}, t)], \quad (\text{C6})$$

the equation for $\delta\chi$ in the s scale defined in (C3) is

$$\left(\frac{\partial}{\partial s} + h_H(s) \mathbf{v}_1 \cdot \nabla \right) \delta\chi(\mathbf{r}, \mathbf{v}, s) = \Lambda(\mathbf{v}_1) \delta\chi(\mathbf{r}, \mathbf{v}, s), \quad (\text{C7})$$

where we have introduced the function $h_H(s) = n_H(0)/n_H(s)$, and the linearized Boltzmann operator

$$\begin{aligned} \Lambda(\mathbf{v}_1)g(\mathbf{v}_1) &= (1-p) \frac{\zeta_n}{\Omega} \int d\mathbf{v}_2 \int d\hat{\sigma} [b_\sigma^{-1} - 1] (1 + \mathcal{P}_{12}) \\ &\times \chi_M(v_1)g(\mathbf{v}_2) - p \zeta_n \chi_M(v_1) \int d\mathbf{v}_2 g(\mathbf{v}_2). \end{aligned} \quad (\text{C8})$$

Let us stress that, although there is an exact mapping for the full nonlinear homogeneous equation between $p=0$ and arbitrary p , no such mapping exists for the linear inhomogeneous Boltzmann equation, Eq. (C7). Then, as in the main text, the possibility of a hydrodynamic description depends on the properties of the linearized Boltzmann operator. Here we will see that it is possible to calculate all the eigenfunctions and eigenvalues of this operator and that there is a region of the parameter p in which we have an appropriate scale separation.

Let us write the linearized Boltzmann operator as

$$\Lambda(\mathbf{v}_1)g(\mathbf{v}_1) = (1-p) \Lambda^E(\mathbf{v}_1)g(\mathbf{v}_1) - p \zeta_n \chi_M(v_1) \int d\mathbf{v}_2 g(\mathbf{v}_2), \quad (\text{C9})$$

where we have introduced the linearized Boltzmann operator for elastic Maxwell particles,

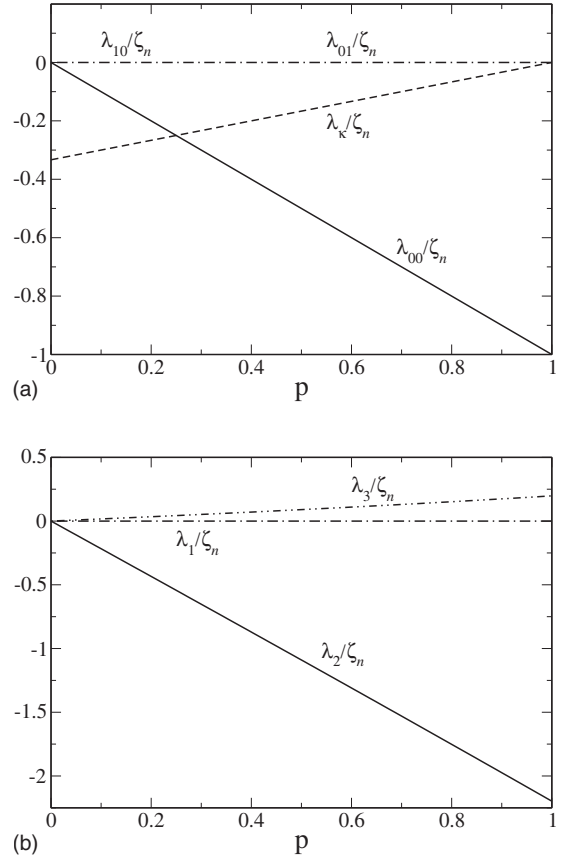


FIG. 8. (a) Hydrodynamic eigenvalues λ_{00} , λ_{10} , and λ_{01} and the slowest kinetic eigenvalue λ_k as a function of the dissipation parameter p . The eigenvalues are normalized by $\zeta_n = \beta\Omega n_H(0)$. (b) Hydrodynamic eigenvalues for hard spheres as a function of the dissipation parameter p .

$$\Lambda^E(\mathbf{v}_1) = \frac{\zeta_n}{\Omega} \int d\mathbf{v}_2 \int d\hat{\sigma} [b_\sigma^{-1} - 1] (1 + \mathcal{P}_{12}) \chi_M(v_1)g(\mathbf{v}_2), \quad (\text{C10})$$

whose spectral properties are well known [27,28]. In particular, for $d=3$ its eigenfunctions are

$$\phi_{rlm}(\mathbf{v}) = A_{rl} \chi_M(v) S_{l+1/2}^r(v^2) v^l Y_{lm}(\theta, \varphi), \quad r = 0, 1, \dots, \quad (\text{C11})$$

where $Y_{lm}(\theta, \varphi)$ are the spherical harmonics, functions of the polar angles (θ, φ) of \mathbf{v} with respect to an arbitrary direction, $S_{l+1/2}^r(v^2)$ are the Sonine polynomials which satisfy

$$\int_0^\infty dx e^{-x} S_q^n(x) S_q^{n'}(x) = \frac{\Gamma(n+q+1)}{n!} \delta_{nn'}, \quad (\text{C12})$$

and A_{rl} are some constants that are introduced in order to normalize the eigenfunctions and that play no role in the following analysis. The eigenvalues of Λ^E and λ_{rl}^E , are also known. It can be seen that λ_{00}^E , λ_{10}^E , and λ_{01}^E (which is three times degenerate) vanish, corresponding to the five hydrodynamic eigenvalues, and that the slowest kinetic mode corresponds to an eigenvalue $\lambda_k^E = -\zeta_n/3$.

The important point here is that the functions ϕ_{rlm} are also eigenfunctions of the second operator in (C9). Taking into account the orthogonality properties of the spherical harmonics and of the Sonine polynomials, Eq. (C12), one has

$$\int d\mathbf{v} \phi_{rlm}(\mathbf{v}) = \delta_{r0} \delta_{l0}. \quad (\text{C13})$$

Then, as $\phi_{000}(\mathbf{v}) = \chi_M(v)$, the functions $\phi_{rlm}(\mathbf{v})$ are in fact the eigenfunctions of the total linearized Boltzmann operator for arbitrary p . With the aid of (C13) is straightforward to see that the eigenvalues are

$$\lambda_{rl} = (1-p)\lambda_{rl}^E - p\zeta_n \delta_{r0} \delta_{l0}. \quad (\text{C14})$$

In Fig. 8 we plot the hydrodynamic eigenvalues as well as the slowest kinetic eigenvalue λ_k as functions of the dissipation parameter p . We have also plotted the hydrodynamic eigenvalues for hard spheres in order to compare both models. It can be seen that for $0 \leq p < 1/4$ there is scale separation in the sense that the three modes (density, linear momentum, and kinetic energy) retained in the coarse-grained description decay more slowly than any of the other kinetic modes. On the other hand, for $1/4 < p \leq 1$, the largest kinetic eigenvalue is slower than λ_{00} . We therefore conclude here that a conservative requirement for the validity of our approach in the case of Maxwell molecules would be $p < 1/4$. Note that a similar breakdown occurs in the inelastic Maxwell model [29,30].

APPENDIX D: EVALUATION OF $\delta\zeta_n$, $\delta\zeta_u$, AND $\delta\zeta_T$

In this appendix we calculate the contribution of the hydrodynamic part of $\delta\chi_k$ to the functionals $\delta\zeta_n$, $\delta\zeta_u$, and $\delta\zeta_T$ defined in (38)–(40). To this end, we write $P\delta\chi_k$ explicitly as

$$\begin{aligned} P\delta\chi_k(\mathbf{c}_1) &= \rho_k \xi_1(\mathbf{c}_1) + \left(\frac{1}{2}\theta_k + \rho_k\right) \xi_2(\mathbf{c}_1) + \mathbf{w}_k \cdot \xi_3(\mathbf{c}_1) \\ &= \rho_k \chi_H(\mathbf{c}_1) - \frac{1}{2}\theta_k \frac{\partial}{\partial \mathbf{c}_1} \cdot [\mathbf{c}_1 \chi_H(\mathbf{c}_1)] - \mathbf{w}_k \cdot \frac{\partial}{\partial \mathbf{c}_1} \chi_H(\mathbf{c}_1). \end{aligned} \quad (\text{D1})$$

Let us first evaluate $\delta\zeta_n[P\delta\chi_k]$. After some algebra it can be seen that

$$\delta\zeta_n[\chi_H(\mathbf{c}_1)] = -4\zeta_n, \quad (\text{D2})$$

$$\delta\zeta_n \left[\frac{\partial}{\partial \mathbf{c}_1} \cdot [\mathbf{c}_1 \chi_H(\mathbf{c}_1)] \right] = 2\zeta_n, \quad (\text{D3})$$

$$\delta\zeta_n \left(\frac{\partial}{\partial \mathbf{c}_1} \chi_H(\mathbf{c}_1) \right) = 0, \quad (\text{D4})$$

where we have used Eqs. (B5) and (B8), the definition of the density decay rate, Eq. (14), and symmetry considerations. Then, if we consider Eqs. (D2)–(D4) we finally obtain

$$\delta\zeta_n[P\delta\chi_k] = -4\zeta_n \rho_k - \zeta_n \theta_k. \quad (\text{D5})$$

Now let us calculate $\delta\zeta_u[P\delta\chi_k]$. Using the definition of the density decay rate, Eq. (14), and symmetry considerations, it appears that

$$\delta\zeta_u[\chi_H(\mathbf{c}_1)] = 0, \quad (\text{D6})$$

$$\delta\zeta_u \left(\frac{\partial}{\partial \mathbf{c}_1} \cdot [\mathbf{c}_1 \chi_H(\mathbf{c}_1)] \right) = 0, \quad (\text{D7})$$

$$\delta\zeta_{u_i} \left(\frac{\partial}{\partial c_{1j}} \chi_H(\mathbf{c}_1) \right) = \delta_{ij} \delta\zeta_{u_i} \left(\frac{\partial}{\partial c_{1i}} \chi_H(\mathbf{c}_1) \right) = 2\zeta_n. \quad (\text{D8})$$

Then we have

$$\delta\zeta_{u_i}[P\delta\chi_k] = -2\zeta_n \mathbf{w}_k. \quad (\text{D9})$$

Finally, we turn to $\delta\zeta_T[P\delta\chi_k]$. Using the definitions of the decay rates, Eqs. (14) and (15), we obtain

$$\delta\zeta_T[\chi_H(\mathbf{c}_1)] = -4\zeta_T, \quad (\text{D10})$$

$$\delta\zeta_T \left(\frac{\partial}{\partial \mathbf{c}_1} \cdot [\mathbf{c}_1 \chi_H(\mathbf{c}_1)] \right) = 6\zeta_T + 4\zeta_n, \quad (\text{D11})$$

$$\delta\zeta_T \left(\frac{\partial}{\partial \mathbf{c}_1} \chi_H(\mathbf{c}_1) \right) = 0, \quad (\text{D12})$$

from which it follows that

$$\delta\zeta_T[P\delta\chi_k] = -4\zeta_T \rho_k - (3\zeta_T + 2\zeta_n) \theta_k. \quad (\text{D13})$$

[1] I. Goldhirsch, *Annu. Rev. Fluid Mech.* **35**, 267 (2003).
[2] J. Dufty, e-print arXiv:0709.0479.
[3] A. Barrat, E. Trizac, and M. H. Ernst, *J. Phys.: Condens. Matter* **17**, S2429 (2005).
[4] J. J. Brey and D. Cubero, in *Granular Gases*, edited by S. Luding and T. Pöschel (Springer, Berlin, 2001).
[5] J. F. Lutsko, *Phys. Rev. E* **72**, 021306 (2005).
[6] E. Ben-Naim, P. Krapivsky, F. Leyvraz, and S. Redner, *J. Chem. Phys.* **98**, 7284 (1994).
[7] R. A. Blythe, M. R. Evans, and Y. Kafri, *Phys. Rev. Lett.* **85**, 3750 (2000).
[8] P. L. Krapivsky and C. Sire, *Phys. Rev. Lett.* **86**, 2494 (2001).

[9] E. Trizac, *Phys. Rev. Lett.* **88**, 160601 (2002).
[10] J. Piasecki, E. Trizac, and M. Droz, *Phys. Rev. E* **66**, 066111 (2002).
[11] A. Lipowski, D. Lipowska, and A. L. Ferreira, *Phys. Rev. E* **73**, 032102 (2006).
[12] S. Chapman and T. G. Cowling, *The Mathematical Theory of Nonuniform Gases* (Cambridge University Press, London, 1960).
[13] F. Coppex, M. Droz, and E. Trizac, *Phys. Rev. E* **70**, 061102 (2004).
[14] J. J. Brey and M. J. Ruiz-Montero, *Phys. Rev. E* **69**, 011305 (2004).

- [15] O. E. Lanford, *Physica A* **106**, 70 (1981).
- [16] F. Coppex, M. Droz, and E. Trizac, *Phys. Rev. E* **69**, 011303 (2004).
- [17] J. J. Brey, J. W. Dufty, and M. J. Ruiz-Montero, in *Granular Gas Dynamics*, edited by T. Pöschel and N. Brilliantov (Springer, Berlin, 2003).
- [18] J. J. Brey and J. W. Dufty, *Phys. Rev. E* **72**, 011303 (2005).
- [19] J. Dufty, e-print arXiv:0707.1111.
- [20] M. P. Allen and D. J. Tildesley, *Computer Simulation of Liquids* (Oxford Science Publications, Bristol, 1987).
- [21] J. J. Brey and M. J. Ruiz-Montero, *Phys. Rev. E* **70**, 051301 (2004).
- [22] J. M. Montanero, A. Santos, and V. Garzó, *Physica A* **376**, 75 (2007).
- [23] V. Garzó, A. Santos, and J. M. Montanero, *Physica A* **376**, 94 (2007).
- [24] J. J. Brey, M. I. García de Soria, and P. Maynar (unpublished).
- [25] J. J. Brey, J. W. Dufty, C. S. Kim, and A. Santos, *Phys. Rev. E* **58**, 4638 (1998).
- [26] A. Santos and J. J. Brey, *Phys. Fluids* **29**, 1750 (1986).
- [27] P. Résibois and M. de Leener, *Classical Kinetic Theory of Fluids* (John Wiley, New York, 1977).
- [28] J. A. McLennan, *Introduction to Nonequilibrium Statistical Mechanics* (Prentice-Hall, Englewood Cliffs, NJ, 1989).
- [29] A. Santos, *Physica A* **321**, 442 (2003).
- [30] V. Garzó and A. Astillero, *J. Stat. Phys.* **118**, 935 (2005).